22 September 1958

Memo To: Professor E. D. Rainville

From: K. M. Siegel

Subject: Recent Publications - Radiation Laboratory

        Enclosed is one copy each of our latest publications

on Radar Cross Sections, Radiation Laboratory Report Nos.

2591-3-T and 2591-4-T. They are forwarded for your informa-

tion.

KMS:hj

Enclosures 2

THE UNIVERSITY OF MICHIGAN

STUDIES IN RADAR CROSS SECTIONS XXVI

Fock Theory

by

R. F. Goodrich

The University of Michigan Report No. 2591-3-T

July 1958

Approved *J. W. Crispin, Jr.*
J.W. Crispin, Jr.
Project Engineer

Engin
&
MR
1657

TABLE OF CONTENTS

PREFACE

This paper is the twenty-sixth in a series growing out of studies of radar cross sections at The University of Michigan Research Institute. The primary aims of this program are:

1.   To show that radar cross sections can be determined analytically.

2. A. To obtain means for computing the radiation patterns from antennas by approximate techniques which determine the pattern to the accuracy required in military problems but which do not require the exact solutions.

  B. To obtain means for computing the radar cross sections of various objects of military interest.

  (Since 2A and 2B are interrelated by the reciprocity theorem it is necessary to solve only one of these problems.)

3.   To demonstrate that these theoretical cross sections and theoretically determined radiation patterns are in agreement with experimentally determined ones.

Intermediate objectives are:

1. A. To compute the exact theoretical cross sections of various simple bodies by solution of the appropriate boundary-value problems arising from electromagnetic theory.

  B. Compute the exact radiation patterns from infinitesimal sources on the surfaces of simple shapes by the solution of appropriate boundary-value problems arising from electromagnetic theory.

  (Since 1A and 1B are interrelated by the reciprocity theorem it is necessary to solve only one of these problems.)

2.   To examine the various approximations possible in this problem and to determine the limits of their validity and utility.

3.   To find means of combining the simple-body solutions in order to determine the cross sections of composite bodies.

4.   To tabulate various formulas and functions necessary to enable such computations to be done quickly for arbitrary objects.

5.   To collect, summarize, and evaluate existing experimental data.

K.M. Siegel

SUMMARY

We present an exposition and certain generalizations of recent work on a class of problems in classical electromagnetic theory. Briefly, we indicate the approach as the Fock theory. It is a method of obtaining the field induced by an incident electromagnetic wave on or near the surface of a good conductor. The surface is restricted to be smooth, convex, and of characteristic dimensions which are "large" with respect to the wavelength of the incident radiation. The term "large" will be made more precise below.

I

TWO DIMENSIONAL PROBLEMS

At the outset we make the point that Fock's method is an essentially two-dimensional method which has as its prototype the solution of the diffraction of electromagnetic radiation by a perfectly conducting, infinite circular cylinder. For this reason we propose to review the solution of the circular cylinder problem. We follow and add somewhat to the treatment of W. Franz (Ref. 1). We consider a perfectly conducting circular cylinder of radius a having its axis along the Z-axis of a Cartesian coordinate system. Let a plane wave be incident along the X-axis.
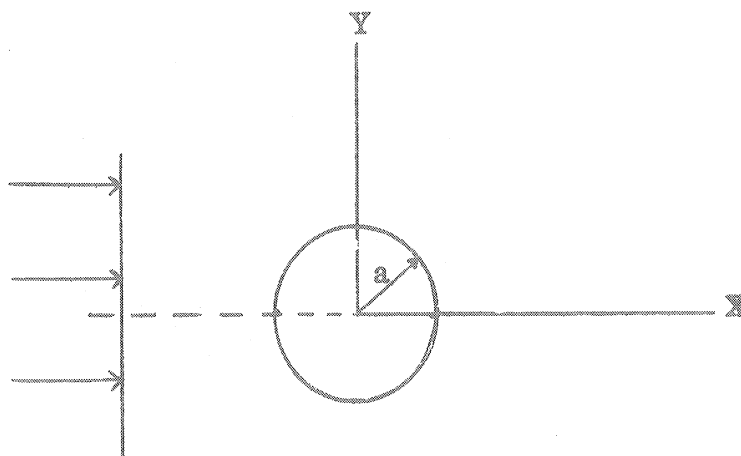
Figure 1.1

We now wish to determine the magnetic field induced on the surface of the cylinder. If the incident magnetic field is in the Z-direction

$$\vec{H}_0 = e^{ikx}\,\hat{z}\ ,\tag{1.1}$$

the only non-vanishing component of the field on the surface is in the Z-direction. Hence, we write

$$\vec{H} = \hat{z}\,\psi\ .\tag{1.2}$$

The function ψ is then required to satisfy the equation

$$(\nabla^2 + k^2)\,\psi = 0\ ,\tag{1.3}$$

where $k = \dfrac{2\pi}{\lambda}$, λ, the wavelength, and the boundary condition

$$\left.\frac{\partial\psi}{\partial r}\right|_{r=a} = 0\ .\tag{1.4}$$

Using a method of R. K. Ritt (Ref. 2) we can immediately write the solution as

$$\psi(a,\phi) = \frac{1}{\pi ka}\int_{-\infty + i\varepsilon}^{\infty + i\varepsilon} d\nu\ \frac{e^{i\nu\left(\phi - \frac{3\pi}{2}\right)} + e^{-i\nu\left(\phi - \frac{\pi}{2}\right)}}{\sin\nu\pi\ H_\nu^{(1)'}(ka)}\ ,\tag{1.5}$$

where ϕ is the polar angle. But since $\text{Im}\,\nu > 0$ we can make the convergent expansion

$$\frac{1}{\sin\nu\pi} = -2i\,e^{i\nu\pi}\sum_{m=0}^{\infty} e^{2i\nu m\pi}\ .\tag{1.6}$$

Substituting in Equation (1.5)

$$\psi = \frac{2i}{\pi ka}\sum_{m=0}^{\infty}\int \frac{d\nu}{H_\nu^{(1)'}(ka)}\left[e^{i\nu(\theta + 2\pi m)} + e^{i\nu(\theta' + 2\pi m)}\right],\tag{1.7}$$

2

where we have put

$$\theta = \phi - \frac{\pi}{2} \, ,$$

$$\theta' = \frac{3\pi}{2} - \phi \quad . \tag{1.8}$$

So, quite generally, we have the problem of solving integrals of the form

$$I(\theta) = \int_{-\infty}^{\infty} d\nu \, \frac{e^{i\nu\theta}}{H_{\nu}^{(1)'}(ka)} \, , \tag{1.9}$$

where θ lies in the range $\left[-\frac{\pi}{2} , \infty \right]$.

We assume $ka \gg 1$ and propose to use certain asymptotic approximations to the Hankel function. The appropriate asymptotic forms are found by an examination of the stationary points of the phase of the integrand.

Using Langer's uniform asymptotic form of the Hankel function (Ref. 3)

$$H_{\nu}^{(1)}(ka) = e^{i\frac{\pi}{6}} \sqrt{\frac{\sin\alpha - \cos\alpha}{\sin\alpha}} \, H_{\frac{1}{3}}^{(1)} \left[ka \, (\sin\alpha - \alpha \cos\alpha) \right] , \tag{1.10}$$

where $\nu = ka \cos\alpha$. We find that the integrand has the phase

$$\phi = \nu\theta - ka \, (\sin\alpha - \alpha \cos\alpha) \quad . \tag{1.11}$$

Hence, the phase is stationary at $\alpha = -\theta$ or

$$\nu = ka \cos\theta \quad . \tag{1.12}$$

We now draw a distinction between the regions $\theta \sim -\frac{\pi}{2}$ and θ near zero or positive. The first region corresponds to the physical region of direct illumination, geometrical optics

region, and by carrying out a stationary phase (Ref. 4) evaluation of the integral we find

$$I(\theta) \tilde{=} \pi \, ka \, e^{ika \sin\theta} \quad . \tag{1.13}$$

So for $\theta \sim -\frac{\pi}{2}$

$$\psi = 2 \, e^{ika \cos\phi} \quad . \tag{1.14}$$

This is just the geometrical optics approximation. The magnetic field induced on the surface is given approximately by twice the tangential component of the incident magnetic field.

For θ near zero we have the condition at the stationary phase point that $\nu \sim ka$ and the Langer form reduces to the Nicholson asymptotic form (Ref. 3) which we write as (Ref. 5)

$$H_\nu^{(1)}(ka) = \frac{-1}{\sqrt{\pi}} \left(\frac{ka}{2}\right)^{-\frac{1}{3}} w(t) \quad , \tag{1.15}$$

where

$$t = \left(\frac{ka}{2}\right)^{-\frac{1}{3}} (\nu - ka) \quad , \tag{1.16}$$

and $w(t)$ is the Airy integral

$$w(t) = \frac{1}{\sqrt{\pi}} \int_\Gamma e^{tZ - \frac{1}{3}Z^3} dZ \quad . \tag{1.17}$$

with the contour Γ given in Figure 1.2. Changing the variable of integration to t

$$I(\theta) = -\pi \, i \, m^3 \, e^{ika \, \theta} \left\{ \frac{1}{\sqrt{\pi}} \int \frac{e^{im\theta t}}{w'(t)} dt \right\} \quad , \tag{1.18}$$

where $m = \left(\frac{ka}{2}\right)^{\frac{1}{3}}$. The integral to be evaluated is then of the form

$$g(\xi) = \frac{1}{\sqrt{\pi}} \int \frac{e^{i\xi t}}{w'(t)} dt \quad , \tag{1.19}$$

where we restrict ξ to be near zero or positive. For $\xi > 0$ $g(\xi)$ can be given as a residue series

$$g(\xi) = \frac{1}{\sqrt{\pi}} \ (2\pi i) \ \sum \frac{e^{i\xi t_n}}{\left. \frac{\partial w'(t)}{\partial t}\right|_{t=t_n}} \quad , \tag{1.20}$$

where

$$w'(t_n) = 0 \quad , \tag{1.21}$$

and we have deformed the contour to encircle the zero of w' which lies in the first quadrant (Ref. 5). For $\xi \sim 0$, however, the residue series converges slowly for $\xi > 0$ and diverges for $\xi < 0$, hence $g(\xi)$ need be found by quadratures.
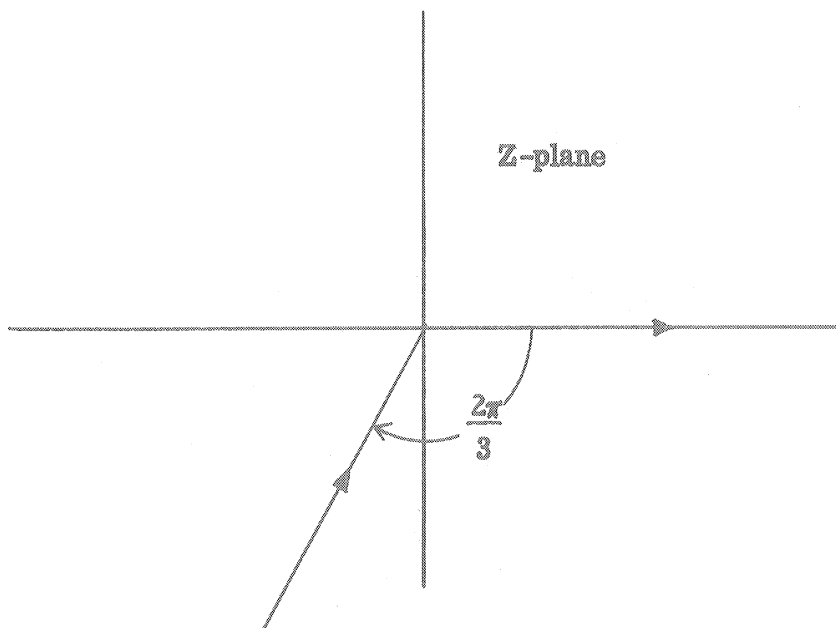

Figure 1.2

The Contour Γ

Substituting in Equation (1.7)

$$\psi_s = \sum_{n=0}^{\infty} \left\{ e^{ikS_n} g(\xi_n) + e^{ikS'_n} g(\xi'_n) \right\} , \qquad (1.22)$$

where we have put

$$S_n = ka (\theta + 2\pi m)$$

$$S_n' = ka (\theta' + 2\pi m) , \qquad (1.23)$$

and

$$\xi_n = \left(\frac{ka}{2}\right)^{\frac{1}{3}} (\theta + 2\pi m)$$

$$\xi_n' = \left(\frac{ka}{2}\right)^{\frac{1}{3}} (\theta' + 2\pi m) . \qquad (1.24)$$

We anticipate the generalization of this approach and note that S_m and S_m' are path lengths on the cylinder surface while ξ_m and ξ_m' are certain reduced distances corresponding to these path lengths.

Finally we give the interpretation of the terms of Equation (1.22) as "creeping waves". We note that the angles θ and θ' measure the angular distance from the geometrical shadow boundaries of cylinder. This is illustrated in Figure 1.3. The interpretation, first proposed by Franz and Deppermann (Ref.6), is that a wave is launched at the shadow boundary and then creeps into the shadow. The subsequent terms in the series with θ replaced by $\theta + 2\pi n$ will then represent terms which have made n circuits around the cylinder. The justification of this interpretation has been given by Friedlander (Ref.7).
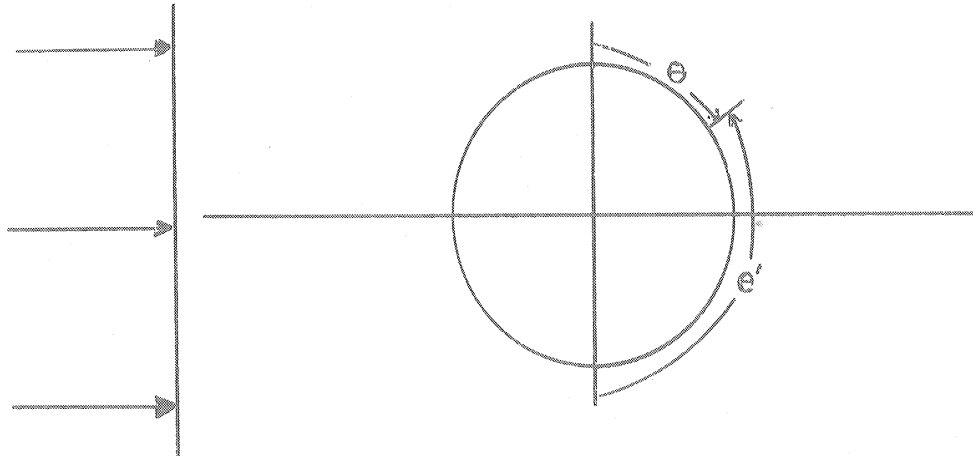
Figure 1.3

For the incident magnetic field along the y-axis we have an analogous treatment.

Briefly, we have on the surface,

$$\vec{H}_s = \hat{\phi} \, X \quad , \tag{1.25}$$

where $\hat{\phi}$ is a unit vector on the surface in the ϕ-direction and

$$X = \frac{1}{\pi m^3} \sum \int d\nu \; \frac{e^{i\nu(\theta+2\pi m)} + e^{i\nu(\theta'+2\pi m)}}{H^{(1)}_{\nu}(ka)} \quad . \tag{1.26}$$

In and near the shadow we approximate the Hankel function by the Airy integral in Equation (1.26) and find

$$X = \frac{1}{m} \sum_n e^{ikS_n} f(\xi_n) \quad ,$$

where S_n and ξ_n are as defined above and

7

$$f(\xi) = \frac{1}{\sqrt{\pi}} \int \frac{e^{i\xi t}}{w(t)} \, dt \; . \tag{1.27}$$

Again, $f(\xi)$ can be evaluated by a residue series for $\xi > 0$ and by quadrature for $\xi \sim 0.'$

For $\xi < 0$, the optics region, the Nicholson approximation to the Hankel function is no longer valid. We use Langer's asymptotic approximation evaluated by stationary phase and find

$$\mathbb{X} \sim 2 \sin \theta \, e^{ikx} \; , \tag{1.28}$$

The "creeping wave" interpretation obtains just as before.

We now give Fock's work (Ref. 8). Fock, by means of a physical argument gives a description of the field in the region of the geometric shadow boundary near the surface in terms of a parabolic differential equation. The import of this in terms of Franz's concept of creeping waves will be made clear below.

We let $f(X, Y) = 0$ be the equation of a convex cylindrical surface, the cylinder axis in the Z-direction. We consider a plane electromagnetic wave to be incident in the X-direction and we take the origin of coordinates to be on the surface at the geometrical shadow boundary, the coordinates given by the solution of $\frac{\partial f}{\partial x} = 0$. This is illustrated in Figure 1.4. Further, we assume a parabolic approximation to the surface, i.e.

$$f(x, y) = y + \frac{1}{2} \frac{x^2}{R_0} \; , \tag{1.29}$$

where R_0 is the radius of curvature at the shadow boundary, the origin of our coordinate system.

8
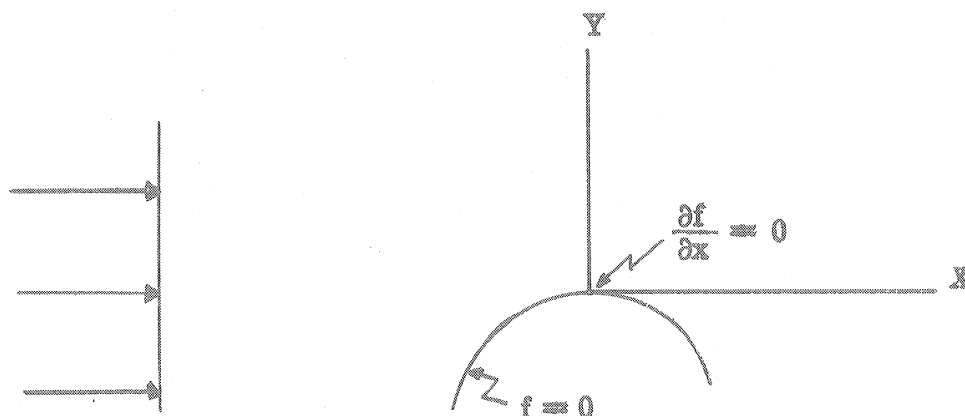
Figure 1.4

This essentially two-dimensional vector problem can be characterized in terms of the scalar problems

$$(\nabla^2 + k^2)\psi = 0 \quad , \tag{1.30}$$

where we assume the time dependence e^{-ikct}. The incident wave will have the functional dependence e^{ikx} and this we introduce explicitly putting

$$\psi = e^{ikx} U \quad . \tag{1.31}$$

Substituting in Equation (1.30) we have

$$U_{xx} + U_{yy} + 2ikU_x = 0 \quad . \tag{1.32}$$

Now we come to Fock's order argument. He supposes that the variation of the functions U in the y-direction, normal to the surface, is greater than the variation in the x-direction. The physical content of this argument is apparent: There is a large variation

in the field quantities on crossing the shadow boundary, $y = 0$, $x > 0$, but having eliminated the dependence on the incident field the variation in the x-direction should be relatively slow.

Fock makes the more precise assumptions

$$\frac{\partial U}{\partial y} = 0 \left(\frac{k}{m} U\right) \quad , \tag{1.33}$$

$$\frac{\partial U}{\partial x} = 0 \left(\frac{k}{M} u\right) \quad , \tag{1.34}$$

where m and M are dimensionless parameters satisfying the inequalities

$$M \gg m \gg 1 \quad . \tag{1.35}$$

Based on this order argument we neglect the second derivative with respect to x in Equation (1.30) and write

$$U_{yy} + 2ikU_x = 0 \quad . \tag{1.36}$$

This implies M is of order m^2 so we put

$$M = m^2 \quad , \tag{1.37}$$

and define the new variables

$$\xi = \frac{mx}{R_0} \quad , \tag{1.38}$$

$$\eta = \frac{2m^2}{R_0} \left(y + \frac{1}{2} \frac{x^2}{R_0}\right) \quad . \tag{1.39}$$

Making the change in variables, Equation (1.32) becomes

$$U_{\eta\eta} + i \frac{kR_0}{2} \frac{1}{m^3} \left(U_\xi + \xi U_\eta\right) = 0 \quad . \tag{1.40}$$

Now choose m such that the coefficient of the last terms becomes one, i.e. put

$$m^3 = \frac{kR_0}{2} \ . \tag{1.41}$$

Equation (1.40) is now

$$U_{\eta\eta} + i(U_\xi + \xi U_\eta) = 0 \ . \tag{1.42}$$

For the purposes of a formal simplification we put

$$U = e^{i\frac{\xi^3}{3} - i\xi\eta} \ V \ . \tag{1.43}$$

This results in the equation

$$V_{\eta\eta} + \eta V + i V_\xi = 0 \ . \tag{1.44}$$

If the incident magnetic field lies in the Z-direction

$$\vec{H}_0 = e^{ikx} \ \hat{z} \ . \tag{1.45}$$

The total field will be of the form

$$\vec{H} = \psi \hat{z} \ , $$

where ψ satisfies Equation (1.30) and the boundary condition

$$\left. \frac{\partial \psi}{\partial n} \right|_{f=0} = 0 \ , \tag{1.46}$$

i.e. the normal derivative of ψ vanishes on the surface. In terms of the function V and the variables ξ, η this condition is

$$\frac{\partial V}{\partial \eta} = 0 \qquad \text{at} \ \eta = 0 \ . \tag{1.47}$$

A particular solution is given by

$$V = e^{i\xi t} \ w(t - \eta) \ , \tag{1.48}$$

11

where $w(t)$ is an Airy integral, the solution of

$$w''(t) = t\,w(t)\ .\tag{1.49}$$

Since two independent solutions are needed we define

$$w_1(t) = \frac{1}{\sqrt{\pi}}\int_{\Gamma_1} e^{Zt-\frac{1}{3}Z^3}\,dZ$$

$$\tag{1.50}$$

$$w_2(t) = \frac{1}{\sqrt{\pi}}\int_{\Gamma_2} e^{Zt-\frac{1}{3}Z^3}\,dZ\ ,$$

where the contours Γ_1 and Γ_2 are given in Figure 1.5. We then look for the solution in
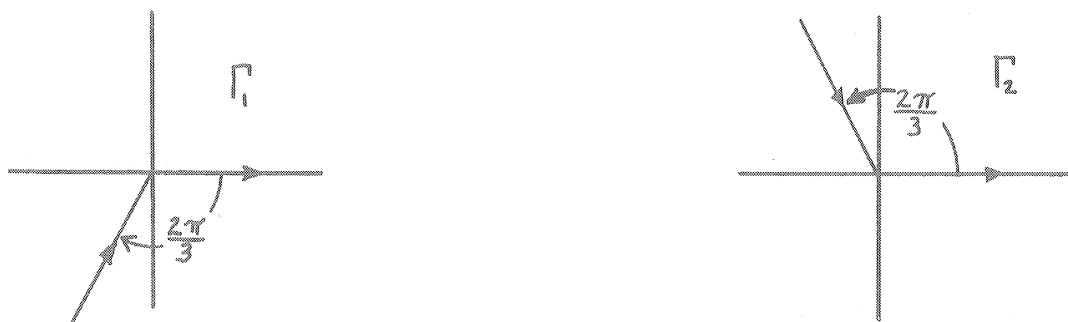

Figure 1.5

the form

$$V = \frac{1}{2\sqrt{\pi}}\int_C e^{i\xi t}\left\{w_2(t-\zeta) - \frac{w_2'(t)}{w_1'(t)}\,w_1(t-\zeta)\right\}dt\ ,\tag{1.51}$$

where we note that this satisfies the differential equation and the boundary condition, and has, from the asymptotic values of the function w_1 and w_2 the correct phase for this problem. The contour C is the same as Γ_3 in Figure 1.5.

The magnetic field is then

$$H_Z = e^{ikx} \; e^{-i\frac{\xi}{3}\zeta \; + i\frac{\zeta^3}{3}} \; v \; , \tag{1.52}$$

or making use of the relationship

$$w_1'(t) \, w_2(t) \; - \; w_1(t) \, w_2'(t) \; = \; -2i \; , \tag{1.53}$$

the field on the surface, $\zeta = 0$, is given by

$$H_Z = e^{ikx} \, G(\xi) \; , \tag{1.54}$$

where

$$G(\xi) = e^{i\frac{\xi^3}{3}} \; \frac{1}{\sqrt{\pi}} \; \int_C dt \; \frac{e^{i\xi t}}{w'(t)} \; . \tag{1.55}$$

For the incident field

$$\vec{H}_0 = \hat{y} \; e^{ikx} \; , \tag{1.56}$$

we have the boundary conditions

$$H_Z = 0 \; , \tag{1.57}$$

and since we confine our attention to the region of the shadow boundary, the normal component of the magnetic field is given by H_y

$$H_y = 0 \quad \text{on} \quad S \; . \tag{1.58}$$

13

Writing as before

$$H_y = e^{ikx} \phi \quad ,$$

ϕ must satisfy

$$\nabla^2 \phi + 2ik \frac{\partial \phi}{\partial x} = 0 \quad , \qquad (1.59)$$

and

$$\phi = 0 \quad \text{on} \quad S \; .$$

We repeat the order argument and write Equation (1.59) as

$$\frac{\partial^2 \phi}{\partial y^2} + 2ik \frac{\partial \phi}{\partial x} = 0$$

$$\qquad (1.60)$$

$$\phi = 0 \quad \text{on} \quad S \; .$$

Now $\vec{H}$ is a divergence-free field

$$\nabla \cdot \vec{H} = 0 \quad , \qquad (1.61)$$

so if we write

$$\vec{H} = e^{ikx} \vec{H^*} \quad , \qquad (1.62)$$

the divergence condition becomes

$$ikH^*_x + \nabla \cdot \vec{H^*} = 0 \; . \qquad (1.63)$$

Repeating the order argument we neglect $\frac{\partial H^*_x}{\partial x}$ as compared with ikH^*_x leaving

$$H^*_x = \frac{1}{k} \frac{\partial H^*_y}{\partial y} \quad , \qquad (1.64)$$

or

$$H^*_x = \frac{1}{m} \frac{\partial \phi}{\partial \eta} \; . \qquad (1.65)$$

14

The field component H_x on the surface is given by

$$H_x = e^{ikx} \frac{1}{m} e^{-i\xi\eta + i\frac{\xi^3}{3}} \frac{\partial \psi}{\partial \eta} \quad , \tag{1.66}$$

where ψ satisfies

$$\psi_{\eta\eta} + \eta\psi + i\psi_\xi = 0$$

$$\psi = 0 \qquad \text{on} \quad S \quad . \tag{1.67}$$

This has a particular solution

$$e^{i\xi t} \, w(t-\xi) \quad . \tag{1.68}$$

So we write

$$\psi = \frac{1}{2\sqrt{\pi}} \int e^{i\xi t} \left\{ w_2(t-\eta) - \frac{w_2(t)}{w_1(t)} \, w_1(t-\eta) \right\} dt \, , \tag{1.69}$$

and

$$\frac{\partial \psi}{\partial \eta}\bigg|_{\eta=0} = \frac{1}{\sqrt{\pi}} \int \frac{e^{i\xi t}}{w(t)} \, dt \quad . \tag{1.70}$$

Using the notation

$$f(\xi) = \frac{1}{\sqrt{\pi}} \int \frac{e^{i\xi t}}{w(t)} \, dt \, , \tag{1.71}$$

we have that on the surface

$$H_x = \frac{1}{m} e^{i\frac{\xi^3}{3}} e^{ikx} \, f(\xi) \quad . \tag{1.72}$$

We are now able to apply Fock's solution to the circular cylinder and compare it with the Franz "creeping wave" solution. From Equations (1.20) and (1.55) we have for the circular cylinder solution and the Fock solution the function

$$g(\xi) = \frac{1}{\sqrt{\pi}} \int \frac{e^{i\xi t}}{w'(t)} \, dt \quad . \tag{1.73}$$

However, we note that for the circular cylinder

$$\xi = \left(\frac{ka}{2}\right)^{\frac{1}{3}} \theta \quad , \tag{1.74}$$

while in the Fock treatment

$$\xi_F = \left(\frac{kR_O}{2}\right)^{\frac{1}{3}} \frac{x}{R_O} \quad , \tag{1.75}$$

or in terms of polar coordinates, since $R_O = a$ and $x = a \sin \theta$

$$\xi_F = \left(\frac{ka}{2}\right)^{\frac{1}{3}} \sin \theta \quad . \tag{1.76}$$

These arguments of the function $g(\xi)$ thus agree to first order for $\theta \sim 0$. This imposes a restriction on the applicability of Fock's method as it stands.

To bring these solutions into agreement we return to the creeping wave interpretation and Fock's derivation of the parabolic differential equation. From the creeping wave interpretation we have a wave launched at the boundary which then creeps <u>along</u> the surface into the shadow boundary. Now the natural description of such a phenomenon would be by a parabolic differential equation. This Fock has done. However, we note that ξ_F measures distance along the direction of propagation rather than along the surface of the obstacle.

We now observe that the argument used by Fock in his derivation of the parabolic equation is also applicable outside the region $\xi \sim 0$ provided we compare the variations

16

of field along the surface of the obstacle and perpendicular to the surface of the obstacle. That is, we can use the Fock equation anywhere in the shadow region provided we define a new set of variables ξ and η for each increment we move into the shadow. To illustrate this we write the formal solution of Equation (1.44) as

$$V(\xi, \eta) = e^{-iT\xi} V(0, \eta) \ , \tag{1.77}$$

where

$$T = -\left(\frac{\partial^2}{\partial \eta^2} + \eta \right) .$$

This gives us an expression valid for say $\xi \leq \xi_1 << 1$. Given this we then redefine our variables and write

$$V(\xi, \eta) = e^{-iT(\xi - \xi_1)} V(\xi_1, \xi) \ , \tag{1.78}$$

which generalizes to

$$V(\xi, \eta) = e^{-iT\xi} V(0, \xi) \ , \tag{1.79}$$

with

$$\xi = \int_0^S \left(\frac{kR(s)}{2} \right)^{\frac{1}{3}} \frac{ds}{R(s)} \ , \tag{1.80}$$

where ds is the element of path length along the surface and R(s) is the radius of curvature at s.

Applying this reasoning to the circular cylinder we have that

$$\xi = \int_0^\theta \left(\frac{ka}{2} \right)^{\frac{1}{3}} \frac{ad\theta}{a} \tag{1.81}$$

$$= \left(\frac{ka}{2} \right)^{\frac{1}{3}} \theta \ . \tag{1.82}$$

This is, however, the expression appearing in Franz's treatment and, hence, we have brought the Franz and Fock solutions into agreement.

17

This important generalization of Fock's work was first found by J. B. Keller (Ref. 9).
Keller proceeds from a local solution of the circular cylinder similar to the above treatment.

We now make a comparison of the Fock result for the circular cylinder with the sum
of the harmonic series as given by L. Bailin (Ref. 10) for ka = 12. In this we use two
"creeping wave" terms.
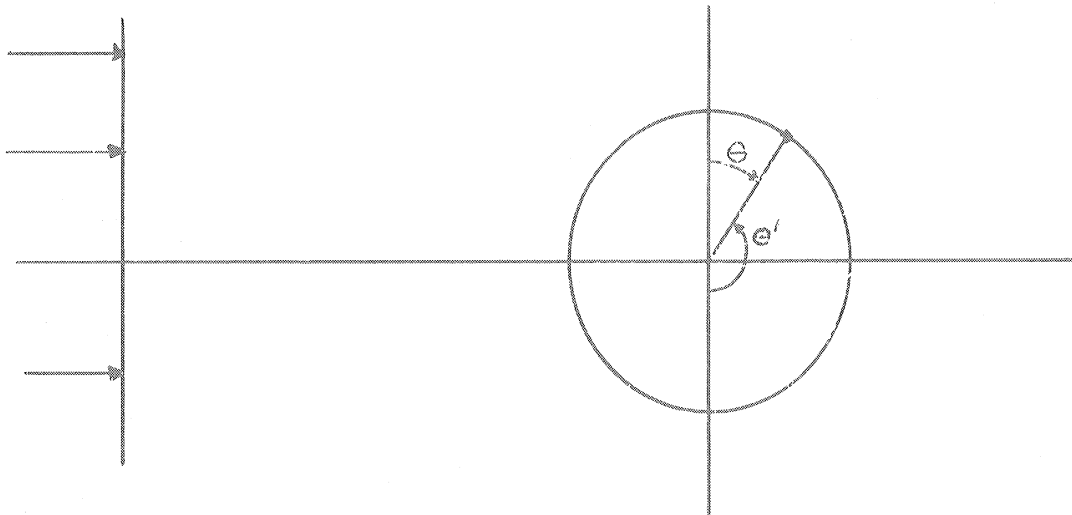
Figure 1.6

At the point θ in Figure 1.6 we determine the contribution arising from the lowest order
terms which "creep" in from each shadow boundary. Then, with the incident magnetic field
parallel to the cylinder axis we have

$$H = e^{ika\,\theta} g\left[\left(\frac{ka}{2}\right)^{\frac{1}{3}} \theta \right]$$
$$+ e^{ika\,\theta'} g\left[\left(\frac{ka}{2}\right)^{\frac{1}{3}} \theta'\right] ,$$

(1.83)

where $\theta' = \pi - \theta$. The comparison is shown in Figure 1.7.

18
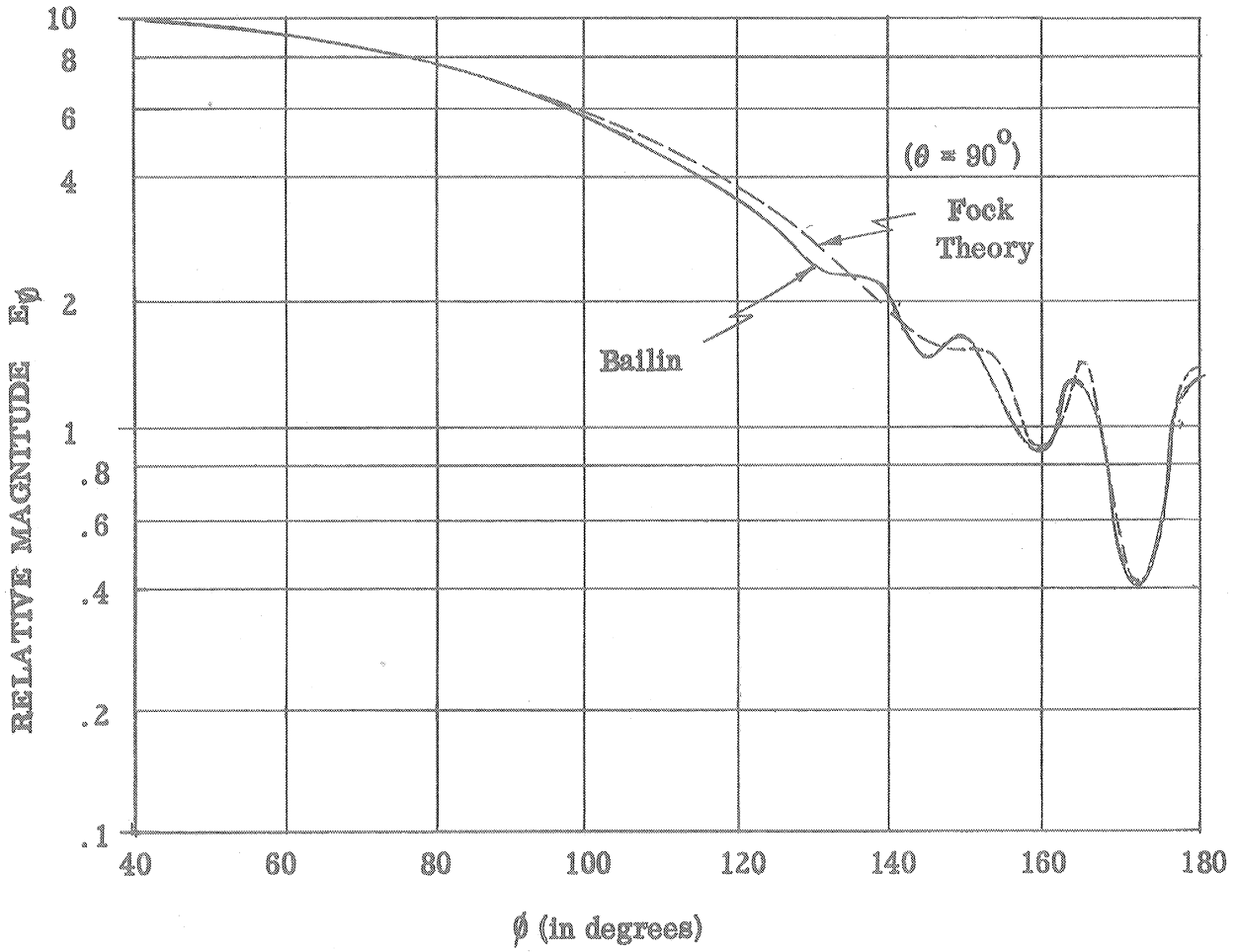
Figure 1.7   COMPARISON OF AMPLITUDES FROM EXACT SERIES AND
FOCK'S CURRENT DISTRIBUTION FOR A CIRCULAR CYLINDER WITH ka = 12

THE UNIVERSITY OF MICHIGAN

As an example of the application of the generalized method we will find the field induced on a perfectly conducting elliptic cylinder by a plane electromagnetic wave. We take the plane wave to be incident along the minor axis of the ellipse with the incident magnetic field parallel to the cylinder axis as in Figure 1.8.
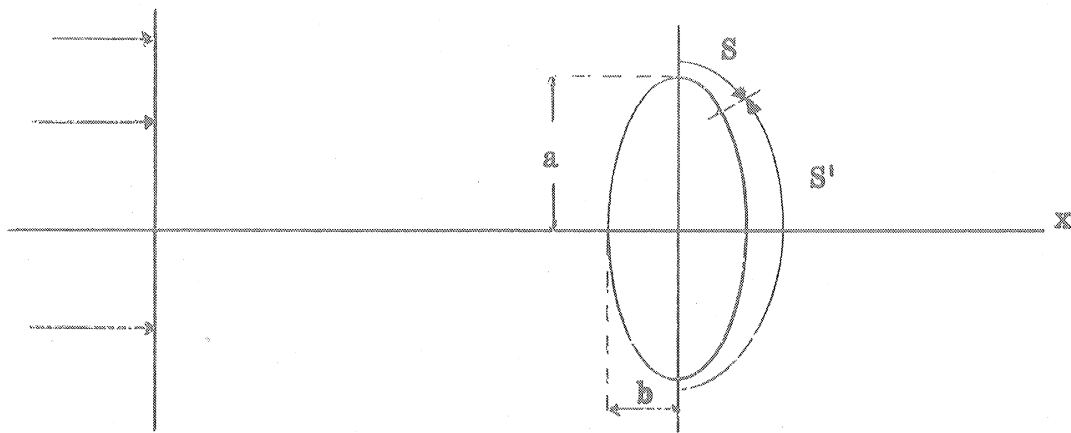
Figure 1.8

If the major and minor semi-axes are a and b respectively the generalized argument of Fock's function is given by

$$\zeta = \int_0^S \left(\frac{kR}{2} \right)^{\frac{1}{3}} \frac{dS}{R}$$

or

$$\zeta = \left(\frac{kb^2}{2a} \right)^{\frac{1}{3}} \left\{ K(\varepsilon) - F(\frac{\pi}{2} - \eta , \varepsilon) \right\} \quad , \tag{1.84}$$

and

$$S = a \left[E(\varepsilon) - E(\frac{\pi}{2} - \eta , \varepsilon) \right] \quad , \tag{1.85}$$

where ε is the eccentricity

$$\varepsilon = \sqrt{1 - \frac{b^2}{a^2}} \quad , \tag{1.86}$$

the parameter η is related to the coordinate by

$$x = b \sin \eta \quad , \tag{1.87}$$

and K and F are elliptic functions of the first kind while E is the elliptic function of the second kind.

$$F(\phi, \varepsilon) = \int_0^\phi \frac{d\phi}{\sqrt{1 - \varepsilon^2 \sin^2 \phi}} \quad , \tag{1.88}$$

$$F(\frac{\pi}{2}, \varepsilon) = K(\varepsilon) \quad , \tag{1.89}$$

$$E(\phi, \varepsilon) = \int_0^\phi \sqrt{1 - \varepsilon^2 \sin^2 \phi} \; d\phi \quad . \tag{1.90}$$

We compute the first two "creeping waves" with

$$S = a(E(\varepsilon) - E(\frac{\pi}{2} - \eta, \varepsilon))$$

$$S' = a(E(\varepsilon) + E(\eta, \varepsilon)) \quad , \tag{1.91}$$

$$\xi = \left(\frac{kh^2}{2a}\right)^{\frac{1}{3}} (K(\varepsilon) - F(\frac{\pi}{2} - \eta, \varepsilon))$$

$$\xi' = \left(\frac{kb^2}{2a}\right)^{\frac{1}{3}} (K(\varepsilon) + F(\eta, \varepsilon)) \quad . \tag{1.92}$$

These arguments give for the shadow region

$$H_z = e^{ikS} g(\xi) + e^{ikS'} g(\xi') \ .$$ (1.93)

We compare this expression with the experiments of Brick and Wetzel (Ref. 11) for

ka = 12 and kb = 7.5 in Figure 1.9.

Keller (Ref. 12) has given a treatment which makes more precise the content of

Fock's assumptions. This method, "the method of stretching", starts from the reduced

equation,

$$\frac{\partial^2 U}{\partial y^2} + \frac{\partial^2 U}{\partial x^2} + 2ik \frac{\partial U}{\partial x} = 0 \ .$$ (1.94)

We introduce the new variables

$$x' = k^\alpha x$$
$$y' = k^\beta y \ ,$$ (1.95)

so that Equation (1.94) becomes

$$k^{2\alpha} U_{x'x'} + k^{2\beta} U_{y'y'} + 2 ik^{\alpha+1} U_{x'} = 0 \ .$$ (1.96)

Now to impose the condition that this goes to Fock's parabolic equation in the limit

$k \to \infty$ we require

$$2\beta = 1 + \alpha > 2\alpha \geq 0 \ .$$

This condition results in the equation

$$V_{y'y'} + 2 i V_{x'} = 0 \ .$$ (1.97)

Again taking the surface to be given by

$$y + \frac{1}{2} \frac{x^2}{a} = 0 \ ,$$ (1.98)

and imposing the Dirichlet boundary condition in the new variables
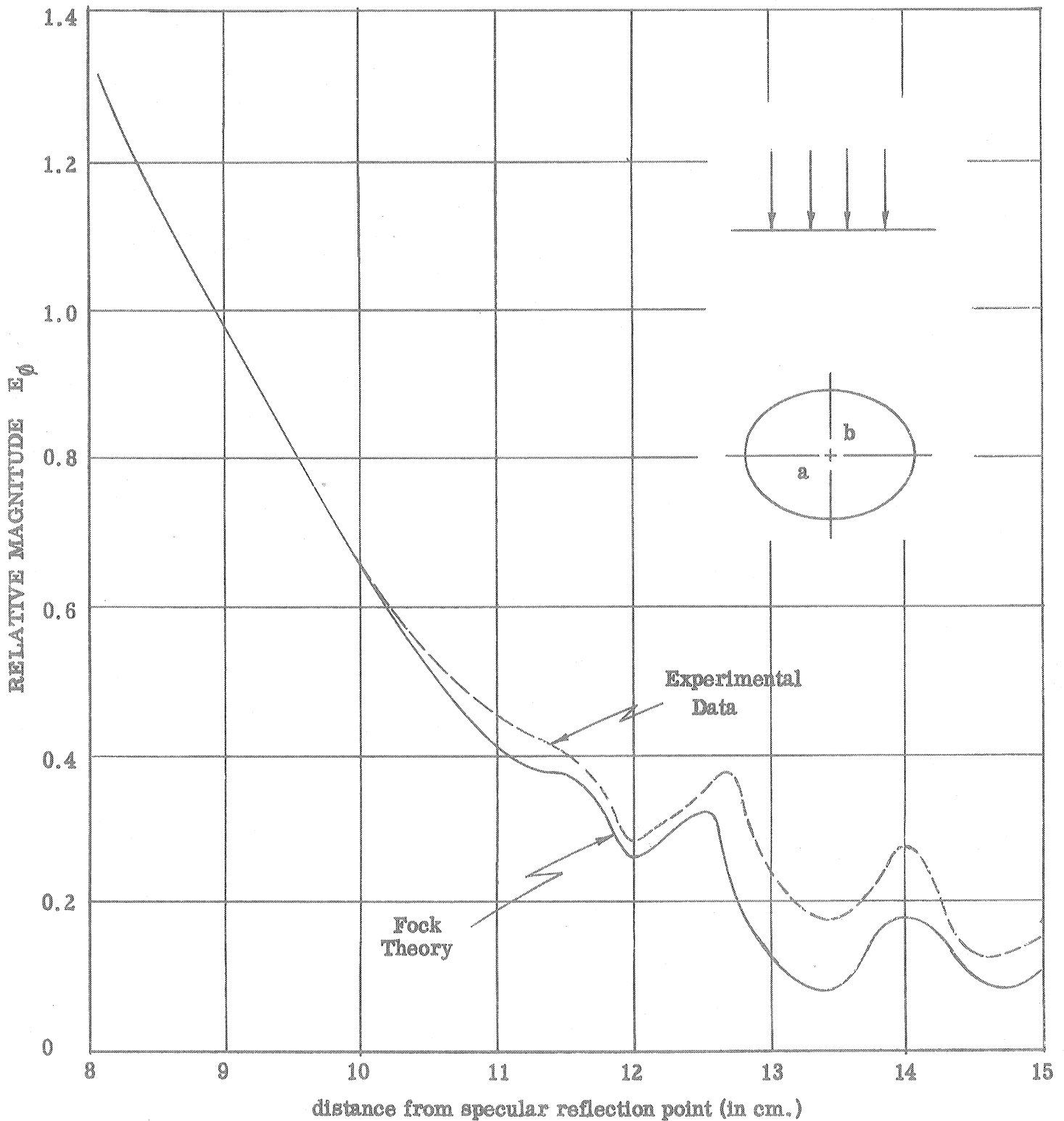
Figure 1.9   COMPARISON OF AMPLITUDES FROM EXPERIMENTAL DATA AND FOCK'S CURRENT DISTRIBUTION FOR AN ELLIPTIC CYLINDER OF ECCENTRICITY 0.780 WITH $ka = 12$ AND $kb = 7.5$

$$V = 0 \quad \text{on} \quad k^{-\beta} y' + k^{-2\alpha} \frac{x'^2}{2a} = 0 \quad . \tag{1.99}$$

Hence, the boundary condition is satisfied on $y' + \frac{1}{2} \frac{x'^2}{a} = 0$ provided

$$\beta = 2\alpha \quad . \tag{1.100}$$

The boundary condition in the limit is then

$$V = 0 \quad \text{on} \quad y' + \frac{1}{2} \frac{x'^2}{a} = 0 \quad \text{for} \quad k \to \infty \quad . \tag{1.101}$$

Solving for α and β

$$\alpha = \frac{1}{3} \quad , \qquad \beta = \frac{2}{3} \quad , \tag{1.102}$$

so the reduced Equation (1.96) becomes

$$U_{y'y'} + 2 i U_{x'} = k^{-\frac{2}{3}} U_{x'x'} \quad . \tag{1.103}$$

Since the solutions of Equations (1.104) and (1.97) cannot be the same function we therefore assume

$$U \sim \sum \frac{U_n}{k^{\lambda n}} \quad . \tag{1.104}$$

Substituting (1.104) in (1.103) U_n must satisfy

$$U_{n_{y'y'}} + 2 i U_{n_{x'}} = - U_{n-1_{x'x'}} \quad , \qquad n > 1 \quad ,$$

$$U_{0_{y'y'}} + 2 i U_{0_{x'}} = 0 \quad , \tag{1.105}$$

and the boundary condition

$$U_n = 0 \quad \text{on} \quad y' + \frac{1}{2} \frac{x'^2}{a} = 0 \quad . \tag{1.106}$$

24

This treatment is, in itself, no greater justification for the Fock method but it does make more precise the meaning of Fock's essentially physically based assumption.

II

THREE DIMENSIONAL PROBLEMS

We now turn to the application of Fock's method to three-dimensional problems. There is an essential complication present in the case of finite, convex, three-dimensional surfaces. Again we will illustrate the general problem by a prototype problem, scalar scattering by a sphere.

We start with the Dirichlet boundary condition, i.e. we wish the solution of

$$(\nabla^2 + k^2)\,\psi \;=\; 0 \tag{2.1}$$

$$\psi\,(a) \;=\; 0 \tag{2.2}$$

where a is the radius of the sphere. In particular we want to determine

$$\left.\frac{\partial\,\psi}{\partial\,r}\right|_{r=a}\,. \tag{2.3}$$

Let the incident field approach along the polar axis then the normal derivative of the field induced on the surface of a sphere of radius a is given by the series

$$\frac{\partial\,\psi_0}{\partial n} \;=\; \sum (n+\tfrac{1}{2})\,P_n(\cos\theta)\,e^{-i\frac{\pi}{2}n}\,\frac{1}{\zeta_n^{(1)}(ka)}\,. \tag{2.4}$$

Since the summand has no singularities with respect to the index on the positive real axis this can be written as the contour integral

$$\frac{\partial\,\psi_0}{\partial n} \;=\;\ldots\; \int_C \nu\,e^{-i\frac{\pi}{2}}\,\frac{1}{\zeta_{\nu-\frac{1}{2}}^{(1)}(ka)}\,\sec\,\nu\,\pi\,P_{\nu-\frac{1}{2}}^*(\cos\theta)\,d\nu \tag{2.5}$$

26

where C is a contour encircling the positive real axis and where we use the notation

$$P^*_{\nu}(x) = P_{\nu}(-x) \ . \tag{2.6}$$

Since the integrand is an odd function of ν regular in the second and fourth quadrants, and having simple poles (the zeros of $\zeta^{(1)}_{-\frac{1}{2}}$ (ka) in the first quadrant) we change the contour C to C_1
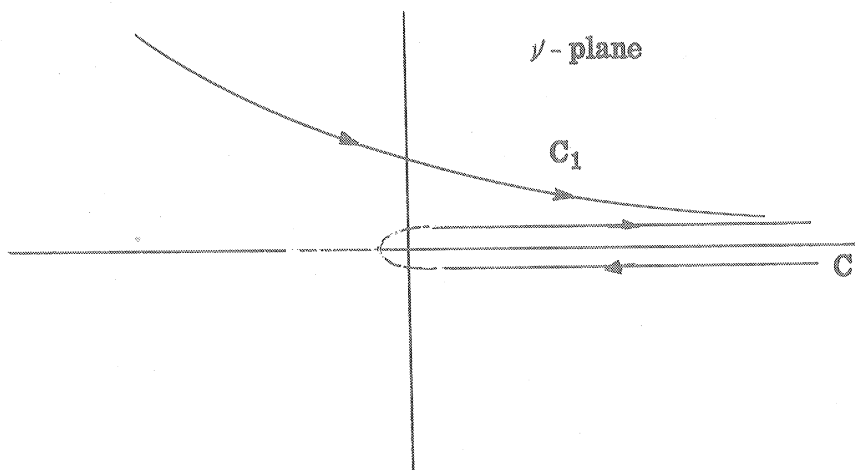
Figure 2.1

Since Im $\nu > 0$ along C_1 we make the convergent expansion

$$Sec \ \nu \pi = e^{i\pi\nu} \sum_{n=0}^{\infty} e^{2\pi i \nu n} (-)^n \ . \tag{2.7}$$

Now making use of the reduction of the Legendre function (Appendix I) we have

$$Sec \ \nu \pi P^*_{\nu-\frac{1}{2}}(\cos\theta) = e^{i\frac{\pi}{2}} \sum (-)^n \left\{ P^{(+)}_{\nu-\frac{1}{2}}(\theta+2\pi n) - P^{(+)}_{\nu-\frac{1}{2}}(2\pi(n+1)-\theta) \right\} \ . \tag{2.8}$$

Substituting in the integrand,

27

$$I(\theta) = e^{i\frac{\pi}{2}} \sum (-)^n \left\{ \int_{C_1} e^{-i\frac{\pi}{2}\nu} \frac{1}{\zeta^{(1)}_{\nu-\frac{1}{2}}(ka)} P^{(+)}_{\nu-\frac{1}{2}}(\theta + 2\pi n) \right. -$$

$$\left. - \int_{C_1} e^{-i\frac{\pi}{2}\nu} \frac{1}{\zeta^{(1)}_{\nu-\frac{1}{2}}(ka)} P^{(+)}_{\nu-\frac{1}{2}}(2\pi(n+1) - \theta) \right\} \tag{2.9}$$

$$I(\theta) = e^{i\frac{\pi}{2}} \sum (-)^n \left\{ I_1(\theta + 2\pi n) - I_1(2\pi(n+1) - \theta) \right\} \tag{2.10}$$

where

$$I_1(\theta) = \int_{C_1} d\nu \frac{e^{-i\frac{\pi}{2}\nu}}{\zeta^{(1)}_{\nu-\frac{1}{2}}(ka)} P^{(+)}_{\nu-\frac{1}{2}}(\theta) . \tag{2.11}$$

For the range $\frac{\pi}{6} < \theta < \frac{5\pi}{6}$ we use the expansion

$$P^{(+)}_{\nu-\frac{1}{2}}(\theta) = \frac{1}{\sqrt{2\pi i \sin\theta}} \frac{\Gamma(\nu+\frac{1}{2})}{\Gamma(\nu+1)} e^{i\nu\theta} F\left(\frac{1}{2}, \frac{1}{2}; \nu+1; \frac{e^{i\theta}}{2i\sin\theta}\right) \tag{2.12}$$

and the notation

$$\phi = \theta - \frac{\pi}{2}, \quad \phi' = \frac{3\pi}{2} - \theta \tag{2.13}$$

so that

$$I(\theta) = \frac{e^{i\frac{\pi}{2}}}{\sqrt{2\pi i \sin\theta}} \sum (-)^n \left\{ \int_{C_1} \frac{\nu \Gamma(\nu+\frac{1}{2})}{\Gamma(\nu+1)} \frac{1}{\zeta^{(1)}_{\nu-\frac{1}{2}}(ka)} \left(e^{i\nu(\phi+2\pi n)} F(\frac{1}{2}, \frac{1}{2}; \nu+1; \right. \right.$$

$$\left. \left. \frac{e^{i\phi}}{2\cos\phi}) - i e^{i\nu(\phi'+2\pi n)} F(\frac{1}{2}, \frac{1}{2}; \nu+1; \frac{e^{i\phi'}}{2\cos\phi'}) \right) \right\} \tag{2.14}$$

28

or defining

$$I_a(\phi) = \int_{C_1} d\nu \; \frac{\Gamma(\nu + \frac{1}{2})}{\Gamma(\nu + 1)} \; \frac{1}{\zeta_{\nu - \frac{1}{2}}^{(1)}(ka)} \; e^{i\nu\phi} \; F\left(\frac{1}{2}, \frac{1}{2}; \nu + 1; \frac{e^{i\phi}}{2\cos\phi}\right) \quad (2.15)$$

we have

$$I(\phi) = \frac{e^{i\frac{\pi}{2}}}{\sqrt{2\pi i \sin\theta}} \sum_{n=0}^{\infty} (-)^n \left\{ I_a(\phi + 2\pi n) - i\, I_a(\phi' + 2\pi n) \right\}. \quad (2.16)$$

The terms of this series correspond to the "creeping waves" of Franz. In this sense we note that ϕ and ϕ' are just the angular distances measured from the shadow boundaries, Figure 2.2.
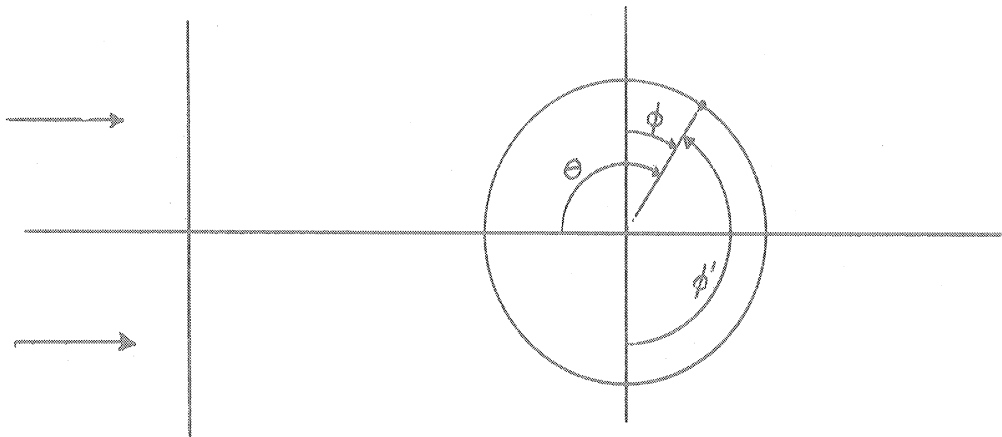
Figure 2.2

The field induced on the surface under the imposition of the Neumann boundary condition follow immediately from the above on the substitution of the derivative of the spherical Hankel function in the denominator of the summand or integrand. We then treat with integrals of the form

$$I_2'(\phi) = \int_{C_1} d\nu \; \frac{\nu \, \Gamma(\nu+\tfrac{1}{2})}{\Gamma(\nu+1)} \; \frac{1}{\zeta_{\nu-\frac{1}{2}}^{\prime (1)}(ka)} \; e^{i\nu\phi} \; F \; . \tag{2.17}$$

We consider the integrals (2.15) and (2.17) in more detail. Assume a sufficiently large value of ka so that the Airy integral approximation for the Hankel function and its derivative is justified. We put e.g.

$$\zeta_{\nu-\frac{1}{2}}^{(1)}(ka) \cong -i \, m^{\frac{1}{2}} \, W(t) \tag{2.18}$$

where

$$m = \left(\frac{ka}{2}\right)^{\frac{1}{3}} \; , \qquad t = \frac{\nu - ka}{m} \; , \tag{2.19}$$

The integral I_2 is then essentially of the form

$$I_2 = \int_{C_2} \phi(t) \; \frac{e^{i\xi t}}{W(t)} \; dt \tag{2.20}$$

where we put $\xi = m\phi$ and C_2 is the contour running from infinity along $\arg t = \frac{2\pi}{3}$ to the origin and from the origin to infinity along $\arg t = 0$.

We note that the form of (2.20) is very like that of Fock's function. In fact, Fock in his paper, Diffraction of Radio Waves Around the Earth's Surface (Ref. 5) arrives at just this form which he then approximates by using the asymptotic form

$$\nu \; \frac{\Gamma(\nu+\tfrac{1}{2})}{\Gamma(\nu+1)} \; F\left(\tfrac{1}{2},\tfrac{1}{2}; \nu+1; \frac{e^{i\theta}}{2i\sin\theta}\right) \sim \sqrt{\nu} \tag{2.21}$$

30

Then, in the shadow region, he evaluates (2.20) as a residue series. Since the first pole occurs near $\nu = ka$, and this for $|ka \sin \theta| >> 1$ is the principal contributor to the residue series, he approximates (2.21) by $\sqrt{ka}$. What remains is precisely one of Fock's functions.

Returning to (2.14) we see that there is an essential difference between the sphere results and the parabolic equation results. The physical significance of this difference is immediate on noting that the parabolic equation is strictly applicable to a two-dimensional problem (the infinite circular cylinder) while the sphere being a finite body forces the waves creeping into the shadow to converge on the pole $\theta = \pi$. This accounts for the term $1/\sqrt{\sin \theta}$ in Equation (2.14). In fact, if we consider that the energy surface density must increase inversely as the available space we have

$$E \sim |\psi|^2 \sim \frac{1}{\sin \theta} \quad , \tag{2.22}$$

or

$$\psi \sim \frac{1}{\sqrt{\sin \theta}} \quad . \tag{2.23}$$

This result has already been noted by Franz (Ref. 1).

N.A. Logan (Ref. 13) has applied Fock's reasoning in approximating the asymptotic form of Equation (2.20) itself. Since the major contribution to the integral comes from the region $t \sim 0$ and $\not p(t)$ is a slowly varying function he writes

31

$$I_2 = \left\{ \int_{C_2} \frac{e^{\frac{1}{3}\xi t}}{W(t)} \, dt \right\} \, \phi(0)$$

(2.24)

$$= \frac{ka \, \Gamma(ka + \frac{1}{2})}{\Gamma(ka + 1)} \, F\left(\frac{1}{2}, \frac{1}{2}; \, ka + 1; \, \frac{e^{i\theta}}{2i \sin \theta} \right) \cdot \int_{C_2} \frac{e^{\frac{1}{3}\xi t}}{W(t)} \, dt \,,$$

where he restricts the region of applicability to $|ka \sin \theta| >> 1$.

Near the pole $\theta = \pi$ we use the asymptotic representation,

$$P^*_{\nu}(\theta) = J_0\left((2\nu + 1) \cos \frac{\theta}{2} \right) + 0\left(\cos^2 \frac{\theta}{2} \right) \,,$$

(2.25)

rather than the decomposition into $P^{(+)}_{\nu}$ and $P^{(-)}_{\nu}$ which are singular at $\theta = \pi$.

Using the above approximations, N. Logan has made a comparison with the sum of the harmonic series for ka = 20 and has found good agreement between the two. In the transition region between $|\nu \sin \theta| >> 1$ and $|\sin \theta| << 1$ the results from either side are continued into this region and even here the agreement was good.

Fock (Ref. 8) has applied his method to the three-dimensional problem. His result is precisely the same as that presented above for the two-dimensional problem.

We consider a finite, smooth, convex, perfectly conducting body illuminated by a plane electromagnetic wave. We take the plane wave to be incident along the x-direction and erect a coordinate system at some point on the shadow boundary with the y-axis normal to the surface and the z-axis chosen so as to form a right-handed system as in Figure 2.3.
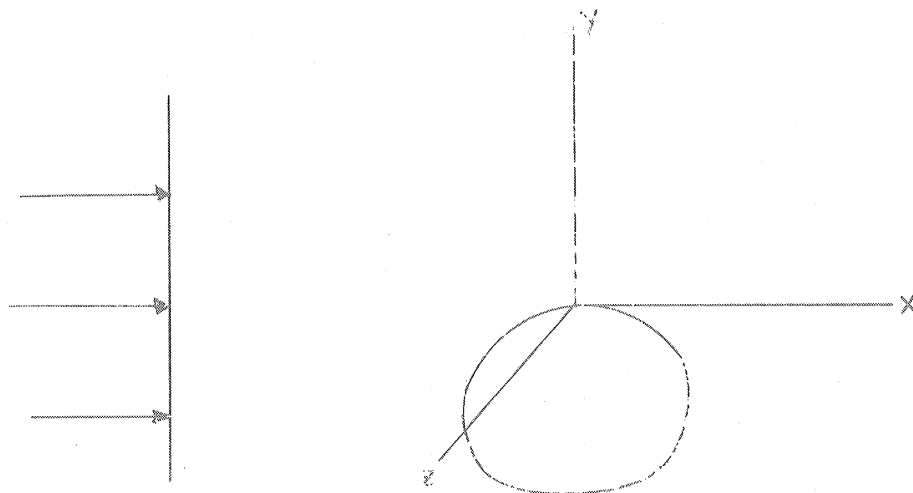
Figure 2.3

As before we perform a local analysis near the origin of the coordinate system. We write

$$\vec{H} = e^{ikx} \vec{H}*$$

$$\vec{E} = e^{ikx} \vec{E}* \quad .$$

(2.26)

Hence, the starred quantities satisfy

$$\nabla x\vec{H}* + ik\hat{x} \times \vec{H}* = -ik \vec{E}*$$

$$\nabla x\vec{E}* + ik\hat{x} \times \vec{E}* = ik \vec{H}* \quad ,$$

(2.27)

from Maxwell's equations for free space.

Now we extend the order argument and write, letting ψ stand for any of the field components, in Equation (2.27),

$$\frac{\partial \Psi}{\partial y} = O\left(\frac{k}{m}\Psi\right) \quad,$$

$$\frac{\partial \Psi}{\partial x} = O\left(\frac{k}{M}\Psi\right) \quad,$$

$$\frac{\partial \Psi}{\partial z} = O\left(\frac{k}{M}\Psi\right) \quad,$$

(2.28)

where, as before,

$$M \gg m \gg 1 \quad,$$

(2.29)

and in fact, we put

$$M = m^2 \quad.$$

(2.30)

Since each of the starred field components must satisfy the reduced wave equation

$$\nabla^2 \Psi + 2ik\frac{\partial \Psi}{\partial x} = 0 \quad,$$

(2.31)

by applying the ordering assumption of Equation (2.31) we have

$$\frac{\partial^2 \Psi}{\partial y^2} + 2ik\frac{\partial \Psi}{\partial x} = 0 \quad.$$

(2.32)

Finally, dropping the asterisks, we have from the ordering assumptions and Equation (2.27)

$$E_x = \frac{1}{k}\left(\frac{\partial H_z}{\partial y} - \frac{\partial H_y}{\partial z}\right) \quad,$$

$$E_y = H_x \quad,$$

$$E_z = -H_y \quad,$$

(2.33)

$$H_x = \frac{1}{k}\left(\frac{\partial H_y}{\partial y} + \frac{\partial H_z}{\partial z}\right).$$

34

We see then that the three-dimensional solutions of Fock are precisely the two-dimensional solutions given above.

In fact for the incident field

$$\vec{H}_o = e^{ikx}\ \hat{z}\ ,\tag{2.34}$$

we put

$$H_x = e^{ikx}\ \psi\ .\tag{2.35}$$

Then, near the shadow boundary, ψ must satisfy

$$\frac{\partial^2 \psi}{\partial y^2} + 2\,ik\,\frac{\partial \psi}{\partial x} = 0\ ,\tag{2.36}$$

and the boundary condition

$$\left.\frac{\partial \psi}{\partial n}\right|_S = 0\ .\tag{2.37}$$

These are precisely the conditions on H_z in the two-dimensional problem as given above in Equation (1.46).

For the incident field

$$\vec{H}_o = e^{ikx}\ \hat{y}\ ,\tag{2.38}$$

on the other hand, we put

$$H_y = e^{ikx}\ \phi\ ,\tag{2.39}$$

where ϕ satisfies

$$\frac{\partial^2 \phi}{\partial y^2} + 2\,ik\,\frac{\partial \phi}{\partial x} = 0\ ,\tag{2.40}$$

$$\left.\phi\right|_S = 0\ .\tag{2.41}$$

These are the conditions given in Equation (1.59) for the two-dimensional problem. Again making use of the divergence condition we have

$$H_x = e^{ikx} \frac{1}{k} \frac{\partial \phi}{\partial y} \; . \tag{2.42}$$

We emphasize that the application of this essentially two-dimensional approach is restricted to the region of the geometric shadow boundary. To carry these solutions farther into the shadow region we must make use of the fact that as the surface area decreases going into the shadow region the energy density must increase. Further, we make the point that the "creeping waves" propagate along geodesics on going into the shadow. The first requirement was illustrated in the treatment of the scalar sphere problem in the appearance of the factor $(\sin \theta)^{-\frac{1}{2}}$ in the expression for the field. The second requirement was met in the tacit assumption that the creeping waves followed great circles on the sphere.

To determine more generally the convergence factor corresponding to $(\sin \theta)^{-\frac{1}{2}}$ in the case of the sphere we consider two adjoining geodesic paths arising on the geometrical shadow boundary. The geodesics are determined by the two conditions:

(1) the point on the shadow boundary at which they arise, and

(2) the angle which the incident radiation makes with the shadow curve.

We write for the two paths

$$\vec{r}_1 = \vec{r} \, (\ell, \, S_1) \; ,$$
$$\vec{r}_2 = \vec{r} \, (\ell + \Delta \ell \, , \, S_2) \; , \tag{2.43}$$

where ℓ and $\ell + \Delta \ell$ are points on the shadow boundary and S_1 and S_2 are path lengths along the geodesics. This is shown in Figure 2.4.
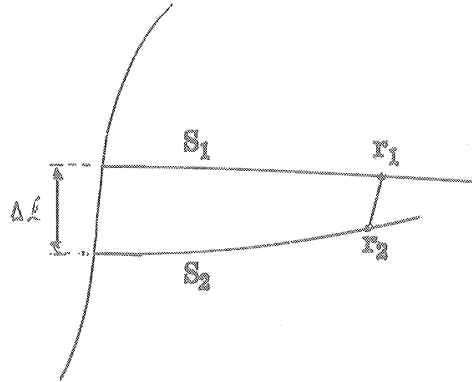
Figure 2.4

We choose S_1 and S_2 so that r_1 and r_2 be equiphase points, then the convergence of area available to the energy propagating into the shadow will be proportional to

$$A = \frac{\vec{r_1} - \vec{r_2}}{\Delta \ell} \quad , \tag{2.44}$$

or in the limit as $\Delta \ell$ vanishes

$$A(\ell, S) = \left| \frac{d\vec{r}(S, \ell)}{d\ell} \right| . \tag{2.45}$$

In order to use the Fock method, then, we require the field functions to be multiplied by the factor $A^{-\frac{1}{2}}$.

III

AN EXAMPLE ; THE CONE

As an illustration of the use of Fock's method for something other than a cylinder or sphere, we now propose to determine the field induced on the surface of a perfectly conducting semi-infinite cone by an incident plane electromagnetic wave. We restrict ourselves to the condition that not all of the cone be illuminated and we shall use Fock's method to find the field on the surface in and near the shadow region.

Here we obtain an approximate method of determining the field on the surface of a perfectly conducting semi-infinite cone which has been illuminated by a plane electromagnetic wave. In particular we take the direction of incidence to be such that not all of the cone surface is illuminated and find the field on that part of the surface which lies in the shadow and which is far from the tip. The approach is that of Franz and Fock generalized after an idea of Keller.

We take a plane electromagnetic wave incident on a perfectly conducting semi-infinite cone. We take the direction of incidence to be such that part of the cone is shadowed and apply the Franz-Fock theory to determine the field induced on the surface of the cone in the shadow and far from the tip. The term "far from the tip" will be made more precise below and indicated as a requirement for the application of the theory.

Using the coordinate system illustrated in Figure 3.1 the equation of the cone can be given as
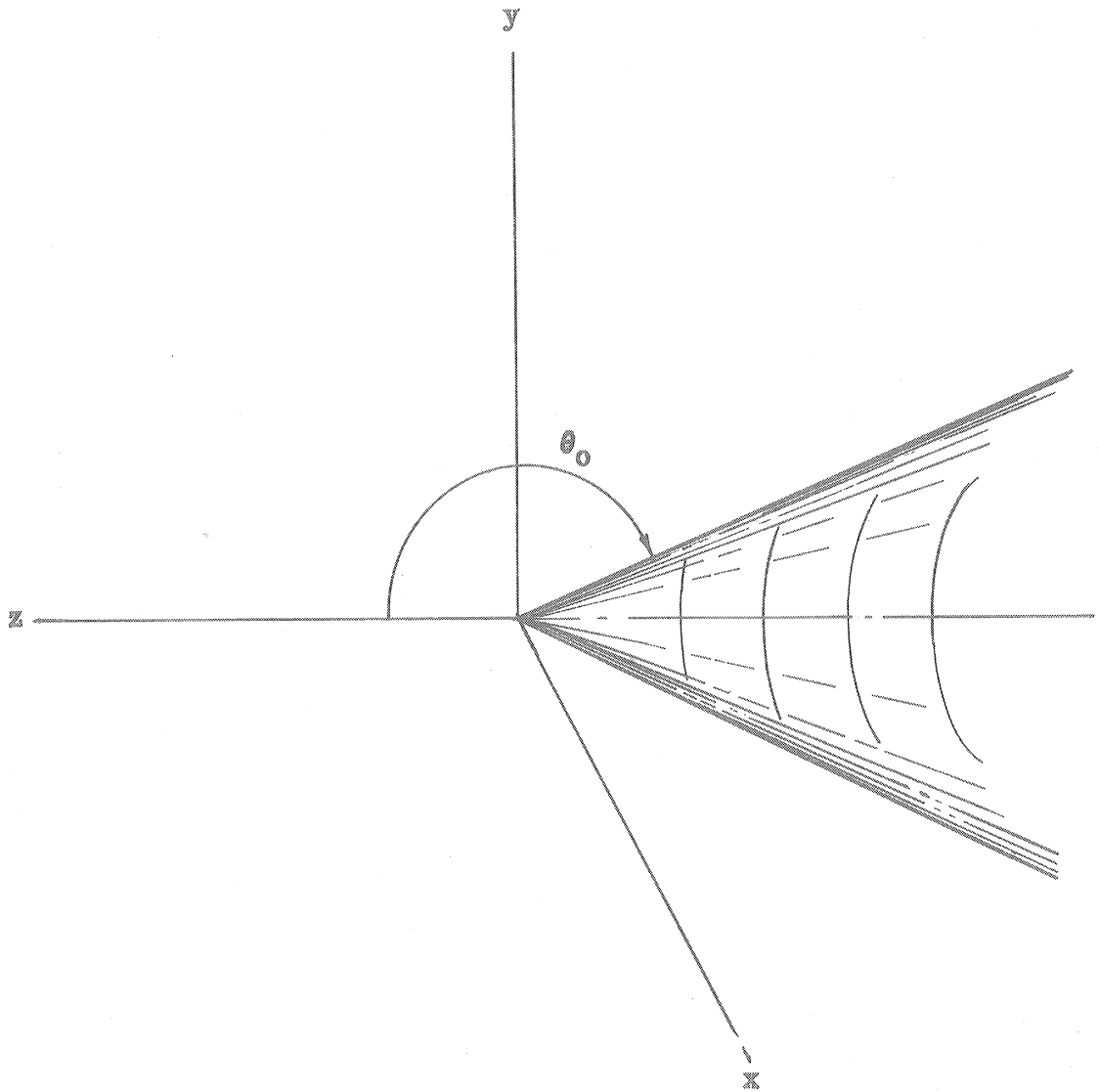
Figure 3.1

Coordinate System for the Cone

$$\theta = \theta_0 , \qquad \theta_0 > \pi/2 . \tag{3.1}$$

The plane wave incident in the xz plane making an angle $\theta(\theta > \pi - \theta_0)$ with the cone axis is again characterized by the unit vector

$$\hat{k} = -\sin\theta\,\hat{i}_x - \cos\theta\,\hat{i}_z . \tag{3.2}$$

This fixes the shadow boundaries which are solutions of

$$\hat{k} \cdot \nabla f = 0 , \tag{3.3}$$

where f = 0 is the equation of the cone, i.e. in Cartesian coordinates

$$f = x^2 + y^2 - z^2 \tan^2\theta_0 . \tag{3.4}$$

Denoting $\phi = \pm\phi_s$ as the equations of the shadow boundaries we have the solutions of (3.3)

$$\cos\phi_s = \frac{\tan\theta_0}{\tan\theta} . \tag{3.5}$$

Taking the viewpoint of Franz we consider the field in the shadow as arising from a wave launched at the shadow boundary and propagating along a geodesic according to the prescription of Fock. This makes more precise the condition on the distance from the tip. We now require the radius of curvature everywhere along the geodesic to be much larger than a wavelength. In Fock's notation

$$\left(\frac{kR}{2}\right)^{\frac{1}{3}} \gg 1 , \tag{3.6}$$

where R is the radius of curvature and $k = \frac{2\pi}{\lambda}$ with λ, the wavelength.

Our first step is to find the geodesics, the curvatures, and finally the generalized arguments of Fock's functions.

We need the equation of the geodesic $\vec{r} = \vec{r}(\phi)$ which starts at some point $r = r_s$, $\phi = \phi_s$ on the shadow boundary and, at this point, has the unit tangent vector $\hat{T} = \hat{k}$. (In this section r will denote radial distance on the surface, primes denoting differentiation.)

The geodesic is given by the equations

$$\hat{r} \cdot \frac{d^2 \vec{r}}{ds^2} = 0 \qquad\qquad r'' - r \sin^2 \theta_o \, \phi'^2 = 0$$

$$\text{or} \qquad\qquad\qquad (3.7)$$

$$\hat{\phi} \cdot \frac{d^2 \vec{r}}{ds^2} = 0 \; , \qquad\qquad r \phi'' + 2 r' \phi' = 0 \; ,$$

where s is the path length along the geodesic and the primes indicate differentiation with respect to s. From the second of Equations (3.7) we have

$$\frac{\phi''}{\phi'} = -2 \frac{r'}{r} \; , \tag{3.8}$$

which has the solution

$$\phi' = \frac{\alpha}{r^2} \; , \tag{3.9}$$

where α is to be determined. Now

$$s = \int_{\phi_s}^{\phi} \left[r^2 \sin^2 \theta_o + \left(\frac{dr}{d\phi}\right)^2 \right]^{\frac{1}{2}} d\phi \; , \tag{3.10}$$

so that

$$\frac{d\phi}{ds} = \phi' = \left[r^2 \sin^2 \theta_o + \left(\frac{dr}{d\phi}\right)^2 \right]^{-\frac{1}{2}} \; . \tag{3.11}$$

41

Equating this to (3.9) we find

$$\frac{dr}{d\phi} = \frac{r}{\alpha} \sqrt{r^2 - \alpha^2 \sin^2 \theta_0} \quad . \tag{3.12}$$

This has the solution

$$r = \alpha \sin \theta_0 \sec \left[(\phi - \phi_s) \sin \theta_0 + \psi \right] \quad , \tag{3.13}$$

where ψ is also to be determined.

Applying the condition $r = r_s$ at $\phi = \phi_s$ we have

$$\alpha = r_s \frac{\cos \psi}{\sin \theta_0} \quad . \tag{3.14}$$

The tangent vector is given by

$$\hat{T} = \frac{d\vec{r}}{ds} = \hat{r} \frac{dr}{ds} + r \frac{d\hat{r}}{ds} \quad , \tag{3.15}$$

which, making use of the above, becomes

$$\tag{3.16}$$
$$\hat{T} = \hat{r} \sin \left[(\phi - \phi_s) \sin \theta_0 + \psi \right] + \hat{\phi} \cos \left[(\phi - \phi_s) \sin \theta_0 + \psi \right] \quad .$$

Now imposing the condition $\hat{T} = \hat{k}$ at $\phi = \phi_s$, $r = r_s$ we have

$$\sin \psi = -\frac{\cos \theta}{\cos \theta_0} \quad . \tag{3.17}$$

Finally

$$r = r_s \cos \psi \sec \left[(\phi - \phi_s) \sin \theta_0 + \psi \right]$$

$$\tag{3.18}$$
$$\psi = \sin^{-1} \left\{ -\frac{\cos \theta}{\cos \theta_0} \right\} \quad .$$

42

The radius of curvature is given by

$$\frac{1}{R} = \left| \frac{d\hat{n}}{ds} \cdot \hat{T} \right| \quad , \tag{3.19}$$

where $\hat{n}$ is the unit normal at the point in question. Since $\hat{n} = \hat{\theta}$,

$$\frac{d\hat{n}}{ds} = - \frac{\cos \theta_0}{\sin \theta_0} \frac{r_s \cos \psi}{r^2} \hat{\phi} \quad . \tag{3.20}$$

Thus, using the above expression for $\hat{T}$,

$$\frac{1}{R} = - \frac{r_s^2}{r^3} \cos^2 \psi \quad \cot \theta_0 \quad . \tag{3.21}$$

We take the generalized argument of the Fock functions in the shadow to be

$$\xi = \int_0^s \left(\frac{kR}{2} \right)^{\frac{1}{3}} \frac{ds}{R} \quad . \tag{3.22}$$

Substituting and performing the integration,

$$\xi = \left(\frac{kr_s}{2} \frac{\cos \psi \sin \theta_0}{\sec^2 \theta_0} \right)^{\frac{1}{3}} (\phi - \phi_s) \quad . \tag{3.23}$$

Finally we anticipate our need for the path length,

$$s = r \sec \psi \quad \sin \left[(\phi - \phi_s) \sin \theta_0 \right] \quad . \tag{3.24}$$

We now apply the Fock theory. We fix on a point r, ϕ in the shadow and determine the contribution to the field at this point arising from the wave launched ar r_s, ϕ_s, where r_s satisfies Equation (3.24) with these fixed r, ϕ.

43

If the incident magnetic field is perpendicular to the surface at r_s, ϕ_s, then, according to Fock, the field at r, ϕ due to the surface wave launched at r_s, ϕ_s will be tangent to the geodesic and given by

$$H_T = e^{iks} \frac{1}{m} f(\xi) \; , \tag{3.25}$$

where s is the path length and

$$m = \left(\frac{kR}{2} \right)^{\frac{1}{3}} , \tag{3.26}$$

$$\xi = \left(\frac{kr_s}{2} \cos \psi \frac{\sin \theta_0}{\sec^2 \theta_0} \right)^{\frac{1}{3}} (\phi - \phi_s) . \tag{3.27}$$

Otherwise, if the incident magnetic field is tangent to the surface at r_s, ϕ_s the field will be perpendicular to the geodesic and given by

$$H_\perp = e^{iks} g(\xi) . \tag{3.28}$$

We need the projection of the magnetic polarization, $\hat{p}$, onto the perpendicular and tangent directions at the shadow boundary in order to apply the above method of computing the field. We designate these directions at the shadow boundary by

$$\begin{aligned}
\hat{q}_\perp &= (\cos \theta_0 \cos \phi_s , \; \cos \theta_0 \sin \phi_s , \; - \sin \theta_0) \\
\hat{q}_{\parallel} &= \hat{q}_\perp \; x \; \hat{k} \; .
\end{aligned} \tag{3.29}$$

Hence, with the incident $\hat{p}$ polarization, the field H_T is multiplied by $(\hat{p} \cdot \hat{q}_\perp)$ while the field $H_\perp$ is multiplied by $(\hat{p} \cdot \hat{q}_{\parallel})$.

There will be a contribution from each geodesic path satisfying the boundary conditions and passing through a given point. We enumerate these.

Let the point in question be specified by r, ϕ where $\phi_s \leq \phi \leq \pi$. Then, given the direction of incidence we have the possible geodesics

$$r = r_s^{(n)} \cos \psi \, \sec \left[(2\pi n + \phi - \phi_s) \sin \theta_0 + \psi \right] , \quad n = 0, 1, \ldots \tag{3.30}$$

$$r = r_s^{(n')} \cos \psi \, \sec \left[(2\pi n' - \phi - \phi_s) \sin \theta_0 + \psi \right] , \quad n' = 1, 2, \ldots \tag{3.31}$$

These are to be solved for $\left\{ r_s^{(n)} \right\}$ and $\left\{ r_s^{(n')} \right\}$, where we note the first set terminates at n such that

$$(2\pi n + \phi - \phi_s) \sin \theta_0 + \psi \geq \frac{\pi}{2} , \tag{3.32}$$

while the second terminates at n' such that

$$(2\pi n' - \phi - \phi_s) \sin \theta_0 + \psi \geq \frac{\pi}{2} , \tag{3.33}$$

corresponding to these will be the sets $\left\{ \xi_n \right\}$ and $\left\{ \xi_{n'} \right\}$ as well as the path lengths $\left\{ s_n \right\}$, $\left\{ s_n' \right\}$.

Since, in general, the shadow boundary does not coincide with the phase front of the incident radiation we take account of the phase by inserting the factor $e^{i\vec{k} \cdot \vec{r}_s^{(n)}}$ or $e^{i\vec{k} \cdot \vec{r}_s^{(n')}}$ in each case. This gives a total phase of

$$\phi_n = \vec{k} \cdot \vec{r}_s(n) + ks^{(n)} , \tag{3.34}$$

$$\phi_{n'} = \vec{k} \cdot \vec{r}_s(n') + ks^{(n')} . \tag{3.35}$$

These are explicitly

$$\phi_n = kr \sin \left[(2\pi n + \phi - \phi_s) \sin \theta_0 + \psi \right] , \tag{3.36}$$

$$\phi_{n'} = kr \sin \left[(2\pi n' - \phi - \phi_s) \sin \theta_0 + \psi \right] .$$

Since we will need to add the various contributions vectorially we choose to facilitate this by resolving the components of the field on the surface in the $\hat{\phi}$ and $\hat{r}$ directions. Now the field H_T lies along the tangent vector

$$\hat{T} = \hat{r} \sin \left[(\phi - \phi_s) \sin \theta_0 + \psi \right] + \hat{\phi} \cos \left[(\phi - \phi_s) \sin \theta_0 + \psi \right] \quad , \qquad (3.37)$$

while the field $H_\perp$ lies along the vector

$$\hat{\theta} \times \hat{T} = -\hat{\phi} \sin \left[(\phi - \phi_s) \sin \theta_0 + \psi \right] + \hat{r} \cos \left[(\phi - \phi_s) \sin \theta_0 + \psi \right] . \qquad (3.38)$$

These explicitly give the $\hat{r}$ and $\hat{\phi}$ components. Finally, we find the total contributions. On the surface at the point r, ϕ we have, for incident polarization $\hat{p}$, $\qquad (3.39)$

$$\vec{H}_1(\hat{p}) = \hat{r} \left[\sum_{n=0} e^{i\bar{\phi}_n} \left\{ (\hat{p} \cdot \hat{q}_{\shortparallel}) g(\xi_n) \cos X_n + (\hat{p} \cdot \hat{q}_\perp)(1/m_n) f(\xi_n) \sin X_n \right\} + \right.$$

$$\left. + \sum_{n'=1} e^{i\bar{\phi}_{n'}} \left\{ (\hat{p} \cdot \hat{q}_{\shortparallel}) g(\xi_{n'}) \cos X_n + (\hat{p} \cdot \hat{q}_\perp)(1/m_{n'}) f(\xi_{n'}) \sin X_{n'} \right\} \right] +$$

$$+ \hat{\phi} \left[\sum_{n=0} e^{i\bar{\phi}_n} \left\{ (\hat{p} \cdot \hat{q}_\perp)(1/m_n) f(\xi_n) \cos X_n - (\hat{p} \cdot \hat{q}_{\shortparallel}) g(\xi_n) \sin X_n \right\} + \right.$$

$$\left. + \sum_{n'=1} e^{i\bar{\phi}_{n'}} \left\{ (\hat{p} \cdot \hat{q}_\perp)(1/m_{n'}) f(\xi_{n'}) \cos X_{n'} - (\hat{p} \cdot \hat{q}_{\shortparallel}) g(\xi_{n'}) \sin X_{n'} \right\} \right] \quad ,$$

where we have put

$$X_n = (2\pi n + \phi - \phi_s) \sin \theta_0 + \psi$$

$$X_{n'} = (2\pi n' - \phi - \phi_s) \sin \theta_0 + \psi \qquad (3.40)$$

A point to note in the case of the cone is that this apparently three-dimensional problem is, away from the tip, and according to the criterion of the Fock method, two-dimensional. This becomes more apparent if we use a geometrical method to find the geodesic paths.

We start by unrolling the cone of angle θ by breaking it at one of the shadow boundaries as in Figure 3.2
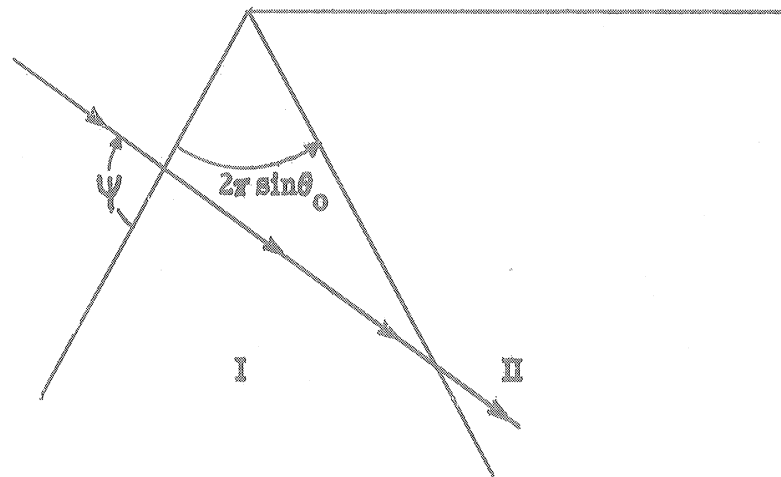
Figure 3.2
The Unrolled Cone

If the incident ray makes an angle ψ with the shadow boundary, this ray continues unchanged onto the unrolled surface. Then we repeat the process and find the rays wrapping around the cone, following geodesic paths are just straight lines.

There is then no convergence or divergence of the geodesics, away from the tip, and this is indeed a two-dimensional problem in the sense of the application of Fock's method.

This method has been used to determine the radiation pattern of an array of slots on a cone. The computation was then compared with experiment and appears in Reference 15. The comparison seems to establish the validity of the Fock approach.

IV

CONCLUSIONS

We can characterize the Fock approach as stemming from a local and primarily physical analysis of the behavior of the fields at and near the geometrical shadow boundary. This coupled with certain general considerations of the known solutions for the circular cylinder, and the sphere give a method of treating the shadow and transition regions provided we exclude any regions in which there is a focussing effect.

Aside from the use of the method in solving physical problems we can look on it as giving a hint as to the form of asymptotic solutions of boundary value problems in which the boundary is a coordinate surface in a system in which the Helmholtz equation is separable. That is to say, we suggest that the asymptotic form of the special functions associated with these separable boundary value problems may be found more easily if we assume the Fock solution is what we are looking for. This approach should be cautious, however, since some recent work of R. K. Ritt (Ref. 2) suggests that there may be a discrepancy in the case of scalar scattering by a prolate spheroid.

Extensive tables of both the Fock functions have been computed by the Air Force Cambridge Research Center under the direction of N. Logan (Ref. 16). These are for positive values of the argument $0 \leqslant \xi \leqslant 9.99$ in steps of 0.01. The function $g(\xi)$ has been computed by Fock (Ref. 14) for $-4.5 \leqslant \xi \leqslant 4.5$ in steps of 0.1.

APPENDIX I

THE CONTINUATION OF CERTAIN SOLUTIONS OF LEGENDRE'S EQUATION TO AN INFINITELY MANY SHEETED RIEMANN SURFACE

For the angular range $\frac{\pi}{6} < \theta < \frac{5\pi}{6}$ we have the representation

$$P_\nu(\cos\theta) = \frac{1}{\sqrt{\pi}} \frac{\Gamma(\ +1)}{\Gamma(\ +\frac{3}{2})} \left\{ e^{i\frac{\pi}{2}} \frac{e^{-i(\nu+\frac{1}{2})\theta}}{\sqrt{2i\sin\theta}} F\left(\frac{1}{2},\frac{1}{2}; \nu+\frac{3}{2}; \frac{-e^{-i\theta}}{2i\sin\theta}\right) + \right.$$

$$\left. + \frac{e^{i(\nu+\frac{1}{2})\theta}}{\sqrt{2i\sin\theta}} F\left(\frac{1}{2},\frac{1}{2}; \nu+\frac{3}{2}; \frac{e^{i\theta}}{2i\sin\theta}\right) \right\}$$

(A.1)

which is absolutely convergent in the specified range. (The series expansion is asymptotic outside this range, i.e. for $\varepsilon < \theta < \pi - \varepsilon$ and $|\nu \sin \varepsilon| \gg 1$). Let $\bar{\xi} \equiv e^{i\theta}$, thus (A.1) becomes

$$P_\nu = \frac{1}{\sqrt{\pi}} \frac{\Gamma(\nu+1)}{\Gamma(\nu+\frac{3}{2})} \left\{ e^{i\frac{\pi}{2}} \frac{\bar{\xi}^{\nu+\frac{1}{2}}}{\sqrt{\xi-\bar{\xi}}} F\left(\frac{1}{2},\frac{1}{2}; \nu+\frac{3}{2}; \frac{-\bar{\xi}}{\xi-\bar{\xi}}\right) + \right.$$

$$\left. + \frac{\xi^{\nu+\frac{1}{2}}}{\sqrt{\xi-\bar{\xi}}} F\left(\frac{1}{2},\frac{1}{2}; \nu+\frac{3}{2}; \frac{\xi}{\xi-\bar{\xi}}\right) \right\}$$

(A.2)

Or equivalently

$$P_\nu = \frac{1}{\sqrt{\pi}} \frac{\Gamma(\nu+1)}{\Gamma(\nu+\frac{3}{2})} \left\{ e^{i\frac{\pi}{2}} \frac{\bar{\xi}^{\nu+1}}{\sqrt{1-\bar{\xi}^2}} F\left(\frac{1}{2},\frac{1}{2}; \nu+\frac{3}{2}; \frac{\bar{\xi}^2}{\bar{\xi}^2-1}\right) + \right.$$

$$\left. + e^{-i\frac{\pi}{2}} \frac{\xi^{\nu+1}}{\sqrt{1-\xi^2}} F\left(\frac{1}{2},\frac{1}{2}; \nu+\frac{3}{2}; \frac{\xi^2}{\xi^2-1}\right) \right\}$$

49

If now we make use of the transformation of the hypergeometric function,

$$F(a, b, c; z) = (1 - z)^{-a} \; F(a, c - b; c; \frac{z}{z - 1}) \quad , \qquad (A.3)$$

Equation (A.2) takes the form

$$P_\nu = \frac{1}{\sqrt{\pi}} \frac{\Gamma(\nu + 1)}{\Gamma(\nu + \frac{3}{2})} \left\{ e^{i \frac{\pi}{2}} \; \tilde{\xi}^{-(\nu+1)} \; F\left(\frac{1}{2}, \nu + 1; \nu + \frac{3}{2}; \tilde{\xi}^2\right) \; + \right.$$

$$\left. + \; e^{-i \frac{\pi}{2}} \; \tilde{\xi}^{-(\nu+1)} \; F\left(\frac{1}{2}, \nu + 1; \nu + \frac{3}{2}; \tilde{\xi}^2\right) \right\} \quad . \qquad (A.4)$$

From this reduction we are led to define the functions

$$P_\nu^{(+)}(\tilde{\xi}) \quad \frac{1}{\sqrt{\pi}} \cdot \frac{\Gamma(\nu + 1)}{\Gamma(\nu + \frac{3}{2})} e^{-i \frac{\pi}{2}} \; \xi^{\nu+1} \quad F\left(\frac{1}{2}, \nu + 1; \nu + \frac{3}{2}; \xi^2\right)$$

$$(A.5)$$

$$P_\nu^{(-)}(\xi) \quad \frac{1}{\sqrt{\pi}} \frac{\Gamma(\nu + 1)}{\Gamma(\nu + \frac{3}{2})} e^{i \frac{\pi}{2}} \; \tilde{\xi}^{\nu+1} \quad F\left(\frac{1}{2}, \nu + 1; \nu + \frac{3}{2}; \tilde{\xi}^2\right).$$

So that

$$P_\nu(\cos \theta) = P_\nu^{(+)} + P_\nu^{(-)} \qquad (A.6)$$

$$P_\nu^*(\cos \theta) = P_\nu(-\cos \theta) = e^{-i \nu \pi} \; P_\nu^{(+)} + e^{i \nu \pi} \; P_\nu^{(-)} \quad .$$

We also note that

$$P_\nu^{(-)}(\theta) = - P_\nu^{(+)}(-\theta) \quad . \qquad (A.7)$$

From the arguments of the hypergeometric functions we have that they are absolutely

convergent on the unit circle except at the points $\tilde{\xi}(\tilde{\xi}) = \pm 1$. They are, moreover,

periodic in θ having the period π so that if we continue the functions $p_\nu^{(\pm)}$ past the cut

$[-1, 1]$ onto an infinitely many sheeted Riemann surface we have

$$p_\nu^{(+)} (\theta + 2\pi n) = e^{2\pi n \nu} \; p_\nu^{(+)} (\theta)$$

$$p_\nu^{(-)} (\theta - 2\pi n) = e^{2\pi n \nu} \; p_\nu^{(-)} (\theta)$$

(A.8)

on the nth sheet.

REFERENCES

1. W. Franz, *Zeit. fur. Natur.* 92, 705 (1954).

2. R.K. Ritt, "Studies in Radar Cross Sections XXX - The Theory of Scalar Diffraction with Application to the Prolate Spheroid", (Appendix by N.D. Kazarinoff), The University of Michigan, Radiation Laboratory Report 2591-4-T, (August 1958). UNCLASSIFIED.

3. Staff of the Bateman Manuscript Project, *Higher Transcendental Functions*, Vol. II, McGraw-Hill (1955).

4. B.L. Van Der Waerden, *Applied Scientific Research*, B2, 33 (1950).

5. V.A. Fock, *Journal of Physics*, IX, 255 (1945).

6. W. Franz and K. Deppermann, *Annalen der Physik*, 10, 361 (1952).

7. F.G. Friedlander, *Communications in Pure and Applied Mathematics*, VII, 705 (1954).

8. V.A. Fock, *Journal of Physics*, X, 399 (1946).

9. J.B. Keller, *Transactions of the Institute of Radio Engineers*, AP-4 312 (1956).

10. L.L. Bailin, *Transactions of the Institute of Radio Engineers*, AP-3 128 (1955).

11. L. Wetzel, D.B. Brick, Air Force Cambridge Research Center, Scientific Report No. 4 (1955).

12. J.B. Keller, private communication.

13. N.A. Logan, private communication.

14. V.A. Fock, *Journal of Physics*, X, 130 (1946).

15. R.E. Doll, R.F. Goodrich, R.E. Kleinman, A.L. Maffett, C.E. Schensted and K.M. Siegel, "Studies in Radar Cross Sections XXVII - Calculated Far Field Patterns from Slot Arrays on Conical Shapes", The University of Michigan, Radiation Laboratory Report 2713-1-F, (February 1958). UNCLASSIFIED.

16. N.A. Logan, Fock Tables (exact title and number to be obtained from AFCRC).

AFCRC DISTRIBUTION LIST

UNIVERSITY OF MICHIGAN – Contract AF19(604)-1949

PART A: CLASSIFIED AND UNCLASSIFIED REPORTS

PART B: FOR UNCLASSIFIED REPORTS ONLY

(one copy unless otherwise noted)

DISTRIBUTION LIST
PART A

CODE	ORGANIZATION
AF 15	Commander Air Research and Development Command Andrew Air Force Base Washington 25, D. C.
AF 29	Commander Eglin Air Force Base Valpariso, Florida
AF 18	Director Air University Library Maxwell Air Force Base, Alabama
AF 5	Commander Air Force Missile Test Center Patrick Air Force Base, Florida ATTN. MU-411 (MTE - CLASSIFIED)
AF 28	Tactical Air Group Directorate of Research and Development, DCS/D Headquarters, USAF Washington, D. C. ATTN: Major R. L. Stell
AF 63	Commander Wright Air Development Center Wright-Patterson Air Force Base, Ohio ATTN: WCLRS-6, Mr. Portune
AF 43	Wright Air Development Center Wright-Patterson Air Force Base, Ohio Flight Research Laboratory, Research Division ATTN: WCRRA
AF 65	Commander Wright Air Development Center Wright-Patterson Air Force Base, Ohio ATTN: WCLNQ-4, N. Draganjac
AF 68	Commander Wright Air Development Center Wright-Patterson Air Force Base, Ohio ATTN: WCLRE-5, Mr. Paul Springer

AF 140   Commander
Air Technical Intelligence Center
Wright-Patterson Air Force Base, Ohio
ATTN: AFCIN-4Bla

AF 141   Commander
Wright Air Development Center
Wright-Patterson Air Force Base, Ohio
ATTN: WCLJH, Dr. C. A. Traenkle

AF 124   Commander
Rome Air Development Center
Griffiss Air Force Base, New York
ATTN: RCSSTL-1

AF 120   Commander
Rome Air Development Center
Griffiss Air Force Base, New York
ATTN: RCUE, Mr. Donald Dakan

AF 139   Commander
Air Force Missile Development Center
Holloman Air Force Base, New Mexico
ATTN: HDOIL, Technical Library

AF 194   Commander
Rome Air Development Center
Griffiss Air Force Base, New York
ATTN: RCEM

AF 195   Commander
Rome Air Development Center
Griffiss Air Force Base, New York
ATTN: RCOPP

AF 196   Commander
Wright Air Development Center
Wright-Patterson Air Force Base, Ohio
ATTN: WCLRE- , Mr. W. F. Bahret

AF 197   Commander
Air Research and Development Command
Andrew Air Force Base
Washington 25, D. C.
ATTN: Col. P. S. Bechtel, RDZPA

AF 198

Commander
Air Force Ballistic Missile Division
Headquarters, ARDC
P. O. Box 262
Inglewood, California
ATTN: WDSIT

AF 199

Commander
Strategic Air Command
Offutt Air Force Base, Nebraska
ATTN: OAET

AF 200

Commander
Air Force Ballistic Missile Division
Headquarters, ARDC
P. O. Box 262
Inglewood, California
ATTN: WDTLAR

AF 205

Defence Research Member
Canadian Joint Staff
2450 Massachusetts Ave., N.W.
Washington 8, D. C.
(for
Defence Research Board, Ottawa, CANADA
ATTN: R. I. Primich
THRU: Commander
        Wright Air Development Center
        Wright-Patterson Air Force Base, Ohio
        ATTN: WCOSR)

AF 201

Operations Analysis Division
Directorate of Operations
Deputy Chief of Staff, Operations
Headquarters, USAF
Washington 25, D. C.
ATTN: Mr. Leroy Brothers

AF 202

Air Defense Command
Headquarters Ent Air Force Base
Colorado Springs, Colorado
ATTN: Lt. Col. Charles Miller

AF 203

Special Projects Branch
Hq. Armed Forces Special Weapons Project
Washington 25, D. C.
ATTN: Lt. Col. R. H. May

AF 204

Office for Development Planning
Deputy Chief of Staff, Development
Headquarters, USAF
Washington 25, D. C.

AR 42

Director
U. S. Army Ordnance
Ballistic Research Laboratories
Aberdeen Proving Ground, Maryland
ATTN: Ballistic Measurements Laboratory

AR 47

Director
Evans Signal Laboratory
Belmar, New Jersey
ATTN: Mr. O. C. Woodyard

AR 5

U. S. Army Signal Research and Development
Laboratories
Evans Signal Laboratory
Belmar, New Jersey
ATTN: Technical Document Center

AR 40

Director
Evans Signal Laboratory
Belmar, New Jersey
ATTN: S. Krevsky, Chief,
Microwave DF and Antenna Section

AR 10

Massachusetts Institute of Technology
Signal Corps Liaison Officer
Cambridge 39, Massachusetts
ATTN: A. D. Bedrosian, Room 26-131

AR 67

Commander
Redstone Arsenal
Huntsville, Alabama
ATTN: Technical Library

AR 76

Operations Research Office
Department of the Army
6410 Connecticut Avenue
Chevy Chase, Maryland
ATTN: Dr. W. W. Nicholas

AR 3

Commander
U.S.A. Signal Engineering Laboratories
Antenna and Microwave Circuitry Section
ATTN: Mr. O. C. Woodyard, Belmar, N. J.

AR 9

Department of the Army
Office of the Chief Signal Officer
Washington 25, D. C.
ATTN: SIGRD-7

AR 41

Department of the Army
Office of Chief Signal Officer
Engineering and Technical Division
Washington 25, D. C.
ATTN: SIGNET-5

AR 39

Commander
U.S. Army Signal Engineering Laboratories
Fort Monmouth, New Jersey
ATTN: Mr. F. J. Triola

AR 48

Diamond Ordnance Fuze Laboratories
Guided Missile Fuze Library
Washington 25, D. C.
ATTN: R. D. Hatcher, Chief
Microwave Development Section

AR 49

Commanding General
U.S. Army Signal Engineering Laboratories
Fort Monmouth, New Jersey
ATTN: SIGFM/EL-AT

G 2

Armed Services Technical Information Agency
Document Service Center
Arlington Hall Station   (8 and master)
Arlington 12, Virginia
ATTN: TICSP

G 6

Office of Technical Services
Department of Commerce   (6)
Washington 25, D. C.
ATTN: Technical Reports Section
(UNCLASSIFIED ONLY)

M 5

Hq Air Force Cambridge Research Center
Air Research and Development Command
Laurence G Hanscom Field
Bedford, Massachusetts
ATTN: CROTRE - P. Condon   (2)

M 6

Hq Air Force Cambridge Research Center
Air Research and Development Command
Laurence G Hanscom Field
Bedford, Massachusetts
ATTN: CROTR - J. Armstrong   (5)

N 1

Director, Avionics Division (AV)
Bureau of Aeronautics
Department of the Navy
Washington 25, D. C.

N 3

Chief, Bureau of Ships
Department of the Navy
Washington 25, D. C.
ATTN: Mr. E. Johnston, Code 833E

N 16

Commander
U. S. Naval Air Missile Test Center
Point Mugu, California
ATTN: Code 366

N 23

U. S. Naval Ordnance Laboratory
White Oak
Silver Spring 19, Maryland
ATTN: The Library

N 26

Commander
U. S. Naval Ordnance Test Station
China Lake, California
ATTN: Code 753

N 28

Air Force Development Field Representative
Naval Research Laboratory
Washington 25, D. C.
ATTN: Code 1072

N 29

Director
U. S. Naval Research Laboratory
Washington 25, D. C.
ATTN: Code 2027

N 30   Dr. J. I. Bohnert, Code 5210
                              U. S. Naval Research Laboratory
                              Washington 25, D. C. [1]

N 35   Commanding Officer and Director
                              U. S. Navy Underwater Sound Laboratory
                              Fort Trumbull, New London, Connecticut

N 37   Chief of Naval Research
                              Department of the Navy
                              Washington 25, D. C.
                              ATTN: Code 427

N 85   Commanding Officer and Director
                              U. S. Navy Electronics Laboratory (Library)
                              San Diego 52, California

N 9   Chief, Bureau of Ordnance
                              Department of the Navy
                              Washington 25, D. C.
                              ATTN: Code Ad3

N 86   Chief, Bureau of Ordnance
                              Department of the Navy
                              Surface Guided Missile Branch
                              Washington 25, D. C.
                              ATTN: Code ReSi-e

N 87   Chief, Bureau of Ordnance
                              Department of the Navy
                              Washington 25, D. C.
                              ATTN: Fire Control Branch (ReS4)

N 88   Department of the Navy
                              Bureau of Aeronautics
                              Technical Data Division, Code 4106
                              Washington 25, D. C.

N 91   Commander
                              U. S. Naval Air Test Center
                              Patuxent River, Maryland
                              ATTN: ET-315, Antenna Branch

N 92   New York Naval Shipyard
                              Material Laboratory, Code 932
                              Brooklyn 1, New York
                              ATTN: Mr. Douglas First

[1]CLASSIFIED REPORTS TO:
   Director, U.S. Naval Research Laboratory, Washington 25, D. C. ATTN: Code 5200

N 93
Director
Naval Ordnance Laboratory
Corona, California

N 97
Commanding Officer
U. S. Naval Ordnance Laboratory
Corona, California
ATTN: Mr. W. Horenstein, Division 72

N 32
Director
U. S. Naval Research Laboratory
Washington 25, D. C.
ATTN: W. S. Arrent, Code 5271

N 131
Chief, Bureau of Ordnance
Navy Department
Washington 25, D. C.

N 132
Chief, Bureau of Ordnance (SP)
Navy Department
Washington 25, D. C.

I 529
Radio Corporation of America
Missile and Surface Radar Department
Moorestown, New Jersey
ATTN: David Shore

I 530
Raytheon Manufacturing Company
P. O. Box 398
Bedford, Massachusetts
ATTN: W. R. Hutchins

I 531
Bell Telephone Laboratories, Inc.
Whippany, New Jersey
ATTN: C. A. Warren

I 532
AVCO Manufacturing Company
20 South Union Street
Lawrence, Massachusetts
ATTN: Henry C. Alberts
        Systems Analysis Group

I 533
AVCO Manufacturing Company
750 Commonwealth Avenue
Boston, Massachusetts
ATTN: Mr. John W. Marchetti

I 534

AVCO Manufacturing Company
2385 Revere Beach Parkway
Everett, Massachusetts
ATTN: Dr. A. R. Kantrowitz

I 535

Ramo-Wooldridge Corporation
Guided Missile Research Division
5760 Arbor Vitae Street
Los Angeles, California
ATTN: F. S. Manov

I 536

General Electric Company
3198 Chestnut Street
Philadelphia 4, Pennsylvania
ATTN: P. R. Gehman, MOSD

I 537

General Electric Company
Electronics Park
Syracuse, New York
ATTN: R. S. Mushrush

I 56

Hughes Aircraft Company
Culver City, California
ATTN: Dr. Van Atta

I 208

Hughes Aircraft Company
Culver City, California
ATTN: D. Adcock

I 538

Battelle Memorial Institute
505 King Avenue
Columbus, Ohio
ATTN: George K. Falkenbach

I 539

Convair, Division of General Dynamics Corp.
San Diego, California
ATTN: Wm. Monroe

I 278

Lockheed Aircraft Corp.
Missile Systems Division
7701 Woodley Avenue
Van Nuys, California

I 541

Cornell Aeronautical Laboratories
4455 Genessee Street
Buffalo 21, New York
ATTN: W. Schatz

I 542

Sylvania Electric Products, Inc.
100 First Street
Waltham, Massachusetts
ATTN: A. Schneider

I 543

Douglas Aircraft Company
Guided Missiles Division
Santa Monica, California
ATTN: J. M. Tachirg

I 544

Missile Section
Bendix Aviation Corporation
400 Beiger Street
Mishawaka, Indiana

I 206

Republic Aviation Corporation
Guided Missiles Division
223 Jericho Turnpike
Mineola, Long Island, New York

I 194

The Rand Corporation
4700 Main Street
Santa Monica, California
ATTN: Dr. A. L. Hiebert

U 220

Columbia University
Electronic Research Laboratory
New York, New York
ATTN: L. O'Neill, Director

U 221

Lincoln Lab., MIT
Box 73
Lexington 73, Massachusetts
ATTN: M. Skolnik

DISTRIBUTION LIST
PART B

CODE

ORGANIZATION

I 1

Airborne Instruments Laboratory, Inc.
160 Old Country Rd., Mineola, N. Y.
ATTN: Dr. E. G. Fubini, Director
Research and Engineering Division

I 8

Bell Aircraft Corporation
P. O. Box 1
Buffalo 5, New York
ATTN: Mrs. J. Mulcahey
   Technical Librarian

I 56

Hughes Aircraft Company
Florence and Teale Sts
Culver City, California
ATTN: Dr. L. C. Van Atta, Associate Director
   Research Laboratories

I 66

The W. L. Maxson Corporation
460 West 34th Street
New York , New York
ATTN: Miss Dorothy Clark

I 82

Northrop Aircraft, Inc.
Hawthorne, California
ATTN: Mr. E. A. Freitas,
   Library Department 3145
1001 E. Broadway

I 96

Sandia Corporation, Sandia Base
P. O. Box 5800, Albuquerque, New Mexico
ATTN: Classified Documents Division

I 116

Melpar, Inc.
3000 Arlington Boulevard
Falls Church, Virginia
ATTN: Engineering Technical Library

I 136

The Glenn L. Martin Company
Rocket Research Library
P. O. Box 179
Denver 1, Colorado
ATTN: Jack McCormick

I 149

Raytheon Manufacturing Co.
Missile Systems Division
Bedford, Massachusetts
ATTN: Mr. Irving Goldstein

I 142

Sanders Associates
95 Canal Street
Nashua, N. H.
ATTN: N. R. Wild, Library

I 126

Convair, A Division of General Dynamics Corp.
Fort Worth, Texas
ATTN: K. G. Brown, Division Research Librarian

I 145

Microwave Radiation Company, Inc.
19223 South Hamilton Street
Gardena, California
ATTN: Mr. Morris J. Ehrlich, President

I 230

Jansky and Bailey, Inc.
1339 Wisconsin Avenue, N. W.
Washington 7, D. C.
ATTN: Mr. Delmer C. Ports

I 233

Radio Corp. of America
RCA Laboratories
Rocky Point, New York
ATTN: P. S. Carter, Lab. Library

I 244

American Machine and Foundry Company
Electronics Division
1085 Commonwealth Avenue
Boston 15, Massachusetts
ATTN: Mrs. Rita Moravcsik, Librarian

I 246

Bendix Aviation Corporation
Pacific Division
11600 Sherman Way
North Hollywood, California
ATTN: J. R. Breninger, Engineering Librarian

I 247

Bendix Radio
Division of Bendix Aviation Corporation
East Joppa Road
Towson 4, Maryland
ATTN: Dr. D. M. Allison, Jr.
        Director of Engineering and Research

I 249

Boeing Airplane Company
Pilotless Aircraft Division
P. O. Box 3707
Seattle 24, Washington
ATTN: R. R. Barber, Library Supervisor

I 250
Boeing Airplane Company
Wichita Division Engineering Library
Wichita 1, Kansas
ATTN: Kenneth C. Knight, Librarian

I 251
Boeing Airplane Company
Seattle Division
Seattle 14, Washington
ATTN: E. T. Allen, Library Supervisor

I 256
Douglas Aircraft Company, Inc.
P. O. Box 200
Long Beach 1, California
ATTN: Engineering Library (C-250)

I 240
Technical Research Group
17 Union Square West
New York, 3, N. Y.
ATTN: M. L. Henderson, Librarian

I 257
Douglas Aircraft Company, Inc.
827 Lapham Street
El Segundo, California
ATTN: Engineering Library

I 258
Douglas Aircraft Company, Inc.
3000 Ocean Park Boulevard
Santa Monica, California
ATTN: P. T. Cline, Eq. Sec. Reference Files
Eq. Eng. A250

I 266
Federal Telecommunication Laboratories
500 Washington Avenue
Nutley 10, New Jersey
ATTN: Technical Library

I 271
Goodyear Aircraft Corp.
1210 Massillon Road
Akron 15, Ohio
ATTN: Library D/120 Plant A

I 207
Hughes Aircraft Company
Antenna Department, Microwave Laboratory
Bldg. 12, Rm 2617
Culver City, California
ATTN: M. D. Adcock

I 280

    The Glenn L. Martin Company
    Baltimore 3, Maryland
    ATTN: Engineering Library,
    Antenna Design Group

I 282

    McDonnell Aircraft Corp.
    Lambert Saint-Louis Municipal Airport
    Box 516, St. Louis 3, Missouri
    ATTN: R. D. Detrich, Engineering Library

I 284

    North American Aviation, Inc.
    12214 Lakewood Boulevard
    Downey, California
    ATTN: Engineering Library 495-115

I 285

    North American Aviation, Inc.
    Los Angeles International Airport
    Los Angeles 45, California
    ATTN: Engineering Technical File

I 289

    Radiation, Inc.
    P. O. Drawer 37
    Melbourne, Florida
    ATTN: Technical Library, Mr. M. L. Cox

I 290

    RCA Laboratories
    David Sarnoff Research Center
    Princeton, New Jersey
    ATTN: Miss Fern Cloak, Librarian,
    Research Library

I 291

    Radio Corporation of America
    Defense Electronic Products
    Bldg. 10, Floor 7
    Camden 2, New Jersey
    ATTN: Mr. Harold J. Schrader, Staff Engineer
           Organization of Chief Technical Administrator

I 292

    Director, USAF Project RAND
    Via: Air Force Liaison Office
    The Rand Corporation
    1700 Main Street
    Santa Monica, California

I 294   Raytheon Manufacturing Company
Wayland Laboratory
Wayland, Massachusetts
ATTN: Miss Alice G. Anderson, Librarian

I 295   Republic Aviation Corporation
Farmingdale, Long Island, New York
ATTN: Engineering Library

Thru: Air Force Plant Representative
       Republic Aviation Corp.
       Farmingdale, Long Island, New York

I 297   Sperry Gyroscope Company
Great Neck, Long Island, New York
ATTN: Florence W. Turnbull, Engr. Librarian

I 298   Stanford Research Institute
Menlo Park, California
ATTN: Library, Engineering Division

I 302   International Business Machines Corp.
Military Products Division
Oswego, New York
ATTN: Mr. D. I. Marr, Librarian
       Dept. 459

I 311   Hycon Eastern, Inc.
75 Cambridge Parkway
Cambridge, Massachusetts
ATTN: Mrs. Lois Seulowitz, Technical Librarian

I 472   Raytheon Manufacturing Company
Missile Division
Hartwell Road
Bedford, Massachusetts

I 374   AVION Division
ACF Industries, Inc.
800 North Pitt Street
Alexandria, Virginia
ATTN: Technical Library

I 472   Raytheon Manufacturing Company
Missile Division
Hartwell Road
Bedford, Massachusetts

I 139

Westinghouse Electric Corp.
Electronics Division
Friendship International Airport
Box 746
Baltimore 3, Maryland

U 3

University of Alaska
Library Geophysical Institute
College, Alaska

U 10

Cornell University
School of Electrical Engineering
Ithaca, New York
ATTN: Prof. G. C. Dalman

U 39

New York University
Institute of Mathematical Sciences
Rm 802, 25 Waverly Place
New York 3, New York
ATTN: Professor Morris Kline

U 45

The Pennsylvania State University
Dept. of Electrical Engineering
University Park, Pa.

U 54

Harvard College Observatory
60 Garden Street
Cambridge 39, Massachusetts
ATTN: Dr. Fred L. Whipple

U 32

Massachusetts Institute of Technology
Research Laboratory of Electronics
Rm 20B-221
Cambridge 39, Massachusetts
ATTN: John H. Hewitt

U 48

Polytechnic Institute of Brooklyn
Microwave Research Institute
55 Johnson Street
Brooklyn, New York
ATTN: Dr. Arthur A. Oliner

U 61

Brown University
Dept. of Electrical Engineering
Providence, R. I.
ATTN: Dr. C. M. Angulo

U 68
    Lowell Technological Institute
    Research Foundation
    P. O. Box 709
    Lowell, Massachusetts
    ATTN: Dr. Charles R. Mingins

U 59
    Library
    Georgia Institute of Technology
    Engineering Experiment Station
    Atlanta, Georgia
    ATTN: Mrs. J. H. Crosland, Librarian

U 78
    Ohio State University Research Foundation
    Ohio State University
    Columbus 10, Ohio
    ATTN: Dr. T. E. Tice
         Dept. of Electrical Engineering

U 86
    University of Florida
    Department of Electrical Engineering
    Gainesville, Florida
    ATTN: Prof. M. H. Latour, Library

U 96
    Northwestern University
    Microwave Laboratories
    Evanston, Illinois
    ATTN: R. E. Beam

U 99
    California Institute of Technology
    1201 E. California Street
    Pasadena, California
    ATTN: I. E. Newlan

U 97
    Polytechnic Institute of Brooklyn
    Microwave Research Institute
    55 Johnson Street
    Brooklyn, New York
    ATTN: Mr. A. E. Laemmel

U 100
    Electronics Research Laboratory
    University of California
    332 Cory Hall, Berkeley 4, California
    ATTN: J. R. Whinnery, Prof.

U 101
    Carnegie Institute of Technology
    Schenley Park
    Pittsburg 13, Pennsylvania
    ATTN: Albert E. Heins

U 102

Harvard University
Technical Reports Collection
Gordon McKay Library, 303A Pierce Hall
Oxford Street, Cambridge 38, Mass.
ATTN: Mrs. E. L. Hufshmidt, Librarian

U 103

University of Illinois
Documents Division Library
Urbana, Illinois

U 104

University of Illinois
College of Engineering
Urbana, Illinois
ATTN: Dr. P. E. Moyes,
          Department of Electrical Engineering

U 105

Applied Physics Laboratory
The Johns Hopkins University
8621 Georgia Avenue
Silver Spring, Maryland
ATTN: Mr. George L. Seielstad

U 109

The University of Oklahoma
Research Institute
Norman, Oklahoma
ATTN: Prof. C. L. Farrar, Chairman,
          Electrical Engineering

U 110

Syracuse University Research Institute
Collendale Campus
Syracuse 10, New York
ATTN: Dr. C. S. Grove, Jr.
          Director of Engineering Research

U 111

The University of Texas
Electrical Engineering Research Laboratory
P. O. Box 8026, University Station
Austin 12, Texas
ATTN: Mr. John R. Gerhardt
          Assistant Director

U 133

University of Washington
Department of Electrical Engineering
Seattle 5, Washington
ATTN: G. Held, Associate Professor

U 157

California Institute of Technology
Jet Propulsion Laboratory
4800 Oak Grove Drive
Pasadena, California
ATTN: I. E. Newlan

U 158

Massachusetts Institute of Technology
Lincoln Laboratory
P. O. Box 73
Lexington 73, Massachusetts
ATTN: Document Room A-229

U 182

Case Institute of Technology
Cleveland, Ohio
ATTN: Prof. S. Seeley

U 183

Columbia University
Department of Electrical Engineering
Morningside Heights
New York, New York
ATTN: Dr. Schlesinger

U 184

Purdue University
Department of Electrical Engineering
Lafayette, Indiana
ATTN: Dr. Schultz

U 185

University of Pennsylvania
Institute of Cooperative Research
3400 Walnut Street
Philadelphia, Pennsylvania
ATTN: Dept. of Electrical Engineering

U 186

University of Tennessee
Ferris Hall
W. Cumberland Avenue
Knoxville 16, Tennessee

U 187

University of Wisconsin
Department of Electrical Engineering
Madison, Wisconsin
ATTN: Dr. Scheibe

U 188

University of Seattle
Department of Electrical Engineering
Seattle, Washington
ATTN: Dr. D. K. Reynolds

U 189

Wayne University
Detroit, Michigan
ATTN: Prof. A. F. Stevenson